People's Democratic Republic of Algeria
Ministry of Higher Education and Scientific Research
CHADLI BENDJEDID UNIVERSITY - EL TARF
FACULTY OF SCIENCE AND TECHNOLOGY
DEPARTMENT OF PHYSICS

MASTER'S THESIS

FIELD: MATERIAL SCIENCE
STREAM: Physics
SPECIALTY: Materials Physics

Topic:

Effect of the Addition of 5% Fe on the Evolution of the Structural and Microstructural Properties of the Nb_2O_5 Compound: Preparation and Characterization

Presented by:
Ikram BOUZIANE

Supervised by:
Dr. Salah HAMDI

Examination Committee:

Name	Role	Rank	Institution
Boutarfa Hayette	Chair	MCA	University of El Tarf
Hamdi Salah	Supervisor	MCA	University of El Tarf
Debboub Salima	Examiner	MCB	University of El Tarf

Academic Year: 2025/2026

Abstract

This work aims to study the effect of adding 5 wt. % iron on the structural and microstructural evolution of niobium pentoxide Nb_2O_5 prepared by high-energy mechanical milling. Nb_2O_5 and Fe powders were mixed in precise proportions and milled for different durations: 0, 1, 3, 6, 12, and 24 hours. The obtained powders were characterized mainly by X-ray diffraction in order to identify the formed phases and follow the evolution of the crystallographic parameters.

The XRD results show that mechanical milling induces significant structural changes in the Nb_2O_5–5%Fe system. The disappearance of the iron peaks after milling indicates the progressive incorporation of Fe ions into the Nb_2O_5 matrix. A systematic shift of the diffraction peaks toward higher angles was observed, confirming the contraction of the crystal lattice. The unit-cell volume decreased by about 4.3%, from 710.11 Å³ to 680.47 Å³ after 24 hours of milling. This contraction is attributed to the forced insertion of Fe^{3+} ions into the niobium oxide lattice and to the internal stresses generated by high-energy impacts.

The microstructural analysis revealed a progressive decrease in crystallite size from 75.163 nm for the unmilled sample to 42.151 nm after 24 hours of milling. At the same time, microstrain and dislocation density increased, indicating the formation of a highly strained nanocrystalline structure. Traces of a secondary $FeNb_2O_6$ phase were detected after 3 hours of milling. These results demonstrate that mechanical milling is an effective method for modifying the structural and microstructural properties of Fe-doped Nb_2O_5, with potential interest for photocatalytic applications under visible light.

Keywords: Nb_2O_5, Fe doping, mechanical milling, X-ray diffraction, microstructure, crystallite size, microstrain, dislocation density.

Résumé

Ce travail a pour objectif d'étudier l'effet de l'addition de 5 % en masse de fer sur l'évolution structurale et microstructurale du pentoxyde de niobium Nb_2O_5 élaboré par broyage mécanique à haute énergie. Les poudres de Nb_2O_5 et de Fe ont été mélangées selon des proportions précises, puis broyées pendant différentes durées : 0, 1, 3, 6, 12 et 24 heures. Les poudres obtenues ont été principalement caractérisées par diffraction des rayons X afin d'identifier les phases formées et de suivre l'évolution des paramètres cristallographiques.

Les résultats de DRX montrent que le broyage mécanique induit des modifications structurales importantes dans le système Nb_2O_5–5%Fe. La disparition des pics du fer après broyage indique l'incorporation progressive des ions Fe dans la matrice de Nb_2O_5. Un déplacement systématique des pics de diffraction vers les grands angles a été observé, confirmant la contraction de la maille cristalline. Le volume de la maille diminue d'environ 4,3 %, passant de 710,11 $Å^3$ à 680,47 $Å^3$ après 24 heures de broyage. Cette contraction est attribuée à l'insertion forcée des ions Fe^{3+} dans le réseau de l'oxyde de niobium ainsi qu'aux contraintes internes générées par les chocs mécaniques de haute énergie.

L'analyse microstructurale révèle une diminution progressive de la taille des cristallites, passant de 75,163 nm pour l'échantillon non broyé à 42,151 nm après 24 heures de broyage. En parallèle, les microdéformations et la densité de dislocations augmentent, indiquant la formation d'une structure nanocristalline fortement contrainte. Des traces d'une phase secondaire $FeNb_2O_6$ ont été détectées après 3 heures de broyage. Ces résultats montrent que le broyage mécanique est une méthode efficace pour modifier les propriétés structurales et microstructurales du Nb_2O_5 dopé au fer, avec un intérêt potentiel pour des applications photocatalytiques sous lumière visible.

Mots-clés : Nb_2O_5 , dopage au fer, broyage mécanique, diffraction des rayons X, microstructure, taille des cristallites, microdéformation, densité de dislocations.

الملخص

يهدف هذا العمل إلى دراسة تأثير إضافة 5% وزناً من الحديد على تطور الخصائص البنيوية والمجهرية لخماسي أكسيد النيوبيومNb_2O_5 المحضر بواسطة الطحن الميكانيكي عالي الطاقة. تم خلط مساحيق Nb_2O_5 و Feبنسب دقيقة، ثم خضعت لعملية الطحن لفترات زمنية مختلفة: 0، 1، 3، 6، 12 و24 ساعة. تمت دراسة المساحيق المحضرة أساساً باستعمال تقنية حيود الأشعة السينية من أجل تحديد الأطوار المتشكلة ومتابعة تطور المعلمات البلورية.

أظهرت نتائج حيود الأشعة السينية أن الطحن الميكانيكي يؤدي إلى تغيرات بنيوية مهمة في النظام Nb_2O_5–5%Fe. كما أن اختفاء قمم الحديد بعد الطحن يدل على الإدماج التدريجي لأيونات الحديد داخل شبكة Nb_2O_5. وقد لوحظ انتقال منتظم لقمم الحيود نحو الزوايا الكبيرة، مما يؤكد حدوث انكماش في الشبكة البلورية. كما انخفض حجم الخلية البلورية بحوالي 4.3%، من 710.11 Å³ إلى 680.47 Å³ بعد 24 ساعة من الطحن. ويرجع هذا الانكماش إلى الإدخال القسري لأيونات Fe^{3+} داخل شبكة أكسيد النيوبيوم، إضافة إلى الإجهادات الداخلية الناتجة عن الصدمات الميكانيكية عالية الطاقة.

أظهرت الدراسة المجهرية انخفاضاً تدريجياً في حجم البلورات من 75.163 nm في العينة غير المطحونة إلى 42.151 nm بعد 24 ساعة من الطحن. وفي المقابل، ازدادت كل من التشوهات المجهرية وكثافة الانخلاعات، مما يدل على تشكل بنية نانوية بلورية ذات إجهادات داخلية عالية. كما تم الكشف عن آثار طور ثانوي $FeNb_2O_6$بعد 3 ساعات من الطحن. تؤكد هذه النتائج أن الطحن الميكانيكي يمثل طريقة فعالة لتعديل الخصائص البنيوية والمجهرية لمركب Nb_2O_5 المطعم بالحديد، مع إمكانية استعماله في تطبيقات التحفيز الضوئي تحت الضوء المرئي.

الكلمات المفتاحيةNb_2O_5 **:**، التطعيم بالحديد، الطحن الميكانيكي، حيود الأشعة السينية، البنية المجهرية، حجم البلورات، التشوهات المجهرية، كثافة الانخلاعات.

Dedication

Dedication to My Resilient Self

To the one who stood firm when everything else seemed to give way...

I dedicate this work to Myself. To the girl who studied the "Physics of Materials" while discovering the true meaning of "Material Strength" within her own soul.

This journey was never easy. It was shaped by long nights in hospital rooms and the cold silence of white walls, where my pain was the only thing louder than my ambition. I dedicate every word of this thesis to the moments I spent balancing textbooks with fatigue, and dreams with reality. In science, we learn that materials reach their greatest strength under extreme pressure—and I have emerged from my struggles like a diamond, refined by the very fire that tried to break me.

To my family, I have always been the "Final Touch" (Musk of the End), the youngest who carried their hopes. Today, I stand as their pride, proving that the smallest element in a structure can often be the most resilient.

I honor my tired body for not giving up, and my soul for always finding the frequency of hope. This degree is not just an academic achievement; it is a testament to a girl who fought a silent war and won.

The dream has crystallized. The journey continues

Acknowledgments

Praise be to Allah, by Whose grace good deeds are accomplished, and praise be to Allah who illuminated our path of knowledge and granted us patience and steadfastness to complete this work after a journey that was anything but easy.

I extend my deepest gratitude and immense appreciation to my honorable supervisor, Professor Dr. Hamdi Saleh, Professor at the Faculty of Science and Technology, Chadli Bendjedid University - El Tarf. He was never sparing with his valuable guidance, sound advice, and patience throughout the preparation of this research. May Allah reward him with the best rewards. I would also like to express my utmost respect and profound thanks to the honorable Chairperson and members of the examination committee for graciously accepting to evaluate and enrich this work with their sound insights.

In a gesture of gratitude, I extend my heartfelt thanks and appreciation to every teacher and professor who left a mark on my path and accompanied me step by step throughout my educational journey; from primary school, through middle school, up to secondary school and university education.

I would especially like to thank my esteemed teacher, Mr. Mourad Ouchtati, my secondary school teacher, who planted the first seed of passion in my heart; it was studying under him that truly marked the beginning of my love for physics. I also express my deepest gratitude and appreciation to Professor Dr. Saidi Khiari, Professor at Chadli Bendjedid University - El Tarf, who played a great role in my university career and never hesitated to encourage and push me forward, serving as the best support and motivator.

To the fountainhead of giving and tenderness, and the secret of my resilience and success in this life; my beloved mother, Souada, and my dear father, Hamida. Thank you for being my true support, my warm refuge, and the prayers that guarded me through every moment of fatigue.

To my family, upon whom I lean and in whom I take pride; my siblings, Ramzi, Meriem, Nihad, and Yassin. Thank you for standing by my side and for your continuous, unwavering support.

To the joy of my heart and the light of my eyes, my dear little nephew, Wassim. You made my dreams grow with your presence, and I pray to Allah that you grow up to pave your own path to success, reaching the highest levels of graduation and excellence, so that I may see you one day at the pinnacle of glory, just as I have always wished for you.

I also extend a special and heartfelt expression of gratitude to everyone who asked about me during my times of illness, and everyone who encouraged me with a kind word or raised their hands in prayer for me in the unseen. Your sincere words and prayers were the fuel that empowered me whenever my strength waned.

To all of them, I dedicate the fruit of this effort and patience.

Contents

Contents

General Introduction..... 2
Chapter I : Mechanical Milling: Fundamentals and Applications..... 5
I- Mechanical Milling..... 5
1. Introduction..... 5
2. Powder Metallurgy and Solid-State Processing..... 5
2.1 Definition of Powder Metallurgy..... 5
2.2 Advantages of Powder Processing Techniques..... 5
2.3 Applications in Advanced Materials..... 6
3. Mechanical Milling..... 6
3.1 Definition and Historical Background..... 6
3.2 Types of Ball Mills..... 7
3.3 Principle of Mechanical Milling..... 9
4. Mechanisms Occurring During Milling..... 11
4.1 Particle Size Reduction..... 11
4.2 Structural Refinement..... 12
4.3 Formation of Solid Solutions..... 13
4.4 Phase Transformation..... 14
4.5 Defect Formation and Strain Accumulation..... 14
5. Parameters Affecting the Milling Process..... 15
5.1 Milling Time..... 15
5.2 Ball-to-Powder Weight Ratio (BPR)..... 15
5.3 Milling Speed..... 16
5.4 Atmosphere (Air, Argon, Vacuum)..... 16
5.5 Type and Size of Milling Balls..... 16
6. Advantages and Limitations of Mechanical Milling..... 18
6.1 Advantages..... 18
6.2 Limitations..... 18
7. Mechanical Milling of Oxide Materials..... 19
II- Fundamental properties..... 21
1. Crystal structure..... 21

Contents

2. Band energy diagram and electrical properties.....22
3. Optical properties.....23
4. Mechanical properties.....23
5. Thermal properties.....24
III. Applications.....25
1. Solar cells and light emitting diodes :.....25
2. Sensing devices :.....25
3. Batteries and supercapacitors :.....26
4. Catalysts :.....27
5. Other applications :.....27
Chapter II : Experimental Procedures.....32
1. Introduction.....32
2. Preparation of Samples.....32
2.1. Characteristics of Starting Materials.....32
2.2. Weighing of Powders.....32
2.3. Mixing and Mechanical Milling.....33
2.4. Pellet Formation.....33
2.5. Thermal Treatment.....35
2.6. Surface Preparation.....36
3. Characterization Techniques.....37
3.1. Structural Study by X-ray Diffraction (XRD).....37
Chapter III : Results and Discussion.....40
1. Introduction.....40
2. X-ray Diffraction Analysis.....41
2.1. Structural Properties.....47
2.2. Microstructural Properties.....48
3. Evolution of Lattice Parameters and Volume.....48
4. Microstructural Analysis.....50
5. Chapter Conclusion.....52
General Conclusions.....55

List of Tables

List of Tables

Table 1 Main milling parameters and their effects..... 17
Table 2 General influence of milling parameters on powder characteristics.....17
Table 3 Main effects of mechanical milling on oxide materials.....20
Table 4 Relevance of milling effects for Nb_2O_5..... 20
Table 5 Characteristics of the starting powders.....32
Table 6 Variation of the interplanar distances dhkl of the most intense peaks as a function of milling time.....44
Table 7 Variation of microstrain as a function of milling time..... 47
Table 8 Dislocation density as a function of milling time.....47
Table 9 Evolution of lattice parameters and volume..... 49
Table 10 D, ε, and δ as a function of milling time.....52

List of Figures

List of Figures

Figure 1 Schematic illustration of the mechanical milling process[5]..... 7
Figure 2 Schematic representation of a planetary ball mill[7].....7
Figure 3 Schematic representation of an attritor mill.[10].....8
Figure 4 Schematic representation of a conventional ball mill[10].....9
Figure 5 Schematic representation of the main stages occurring during mechanical milling, including fracturing, cold welding, and repeated deformation.[13]..... 10
Figure 6 Evolution of particle size distribution parameters as a function of size reduction[15] 12
Figure 7 Evolution of crystallite size and lattice strain as a function of milling time[18]..... 13
Figure 8 balance.....33
Figure 9 Hydraulic press used for pellet preparation.....34
Figure 10 Cylindrical pellets obtained after uniaxial pressing..... 34
Figure 11 Manual polishing machine used for sample preparation.....36
Figure 12 Bruker D8 Advance X-ray diffractometer used for structural analysis.....37
Figure 13 Schematic representation of X-ray diffraction by a crystalline lattice.....38
Figure 14 : Diffraction pattern of an unmilled Nb_2O_5–5% Fe sample.....41
Figure 15 Diffraction patterns of Nb_2O_5–5% Fe samples milled from 0 to 24 h..... 43
Figure 16 Evolution of the most intense peaks as a function of milling time..... 45
Figure 17 Evolution of the most intence diffraction peaks as a function of milling time..... 46
Figure 18 Variations in the lattice parameters of the T-Nb2O5 phase as a function of milling time..... 49
Figure 19 Evolution of average crystallite as a function of milling time..... 50
Figure 20 Evolutions (a) microstrain (ε ou $<\sigma 2>^{1/2}$ (%)) , et (b) dislocations density δ (m^{-2}) in Nb_2O_5-5%Fe phases as a fonction of milling time..... 51

List of Abbreviations

List of Abbreviations

Abbreviation / Symbol	Meaning
Nb_2O_5	niobium pentoxide
Fe	iron
Nb_2O_5–5%Fe	niobium pentoxide doped with 5 wt.% iron
Fe^{3+}	ferric ion
Nb^{5+}	niobium ion
$FeNb_2O_6$	iron niobium oxide
TiO_2	titanium dioxide
ZnO	zinc oxide
HF	hydrofluoric acid
XRD	x-ray diffraction
DRX	diffraction des rayons x / x-ray diffraction
W–H	williamson–hall method
JCPDS	joint committee on powder diffraction standards
FWHM	full width at half maximum
BPR	ball-to-powder weight ratio
SEM	scanning electron microscopy
MEB	microscopieélectronique à balayage
EDX	energy dispersive x-ray spectroscopy
UV–Vis	ultraviolet–visible spectroscopy
XPS	x-ray photoelectron spectroscopy
XAFS	x-ray absorption fine structure
DSSCs	dye-sensitized solar cells
LEDs	light-emitting diodes
LIBs	lithium-ion batteries
FETs	field-effect transistors
MEMS	micro-electro-mechanical systems
ODH	oxidative dehydrogenation
rpm	revolutions per minute
wt.%	weight percentage
h	hour
nm	nanometer
Å	angstrom
°C	degree celsius
eV	electronvolt
Eg	optical band gap energy
2θ	diffraction angle
θ	bragg angle
λ	x-ray wavelength
β	peak broadening
D	average crystallite size
K	shape factor
ε	microstrain
δ	dislocation density
d_{hkl}	interplanar spacing

List of Abbreviations

V	unit cell volume
a, b, c	lattice parameters
V_O	oxygen vacancy
T-Nb_2O_5	orthorhombic phase of niobium pentoxide
TT-Nb_2O_5	low-temperature phase of niobium pentoxide
H-Nb_2O_5	high-temperature phase of niobium pentoxide

General Introduction

General Introduction

As one of the transition metal oxides, niobium pentoxide (Nb_2O_5) offers a broad variety of properties that make it a potentially useful and highly applicable material in many different areas. In comparison to many other transition metal oxides, Nb_2O_5 has received relatively little attention, which presents a significant opportunity for future investigations aimed at fundamentally understanding this material and finding new and interesting application for it **[1].**

For example, it is a priority to develop highly efficient visible light photocatalysts to realize the practical applications of photocatalysis in industry. Niobium pentoxide (Nb_2O_5) is considered a potentially interesting candidate for the photodegradation of organic pollutants induced by visible light.

Among a variety of semiconductor photocatalysts, niobium pentoxide (Nb_2O_5), as an n-type photocatalyst, has many unique physicochemical properties, including excellent chemical and thermal stability and relatively high photocatalytic activity, making it a suitable photocatalyst for photodegradation **[2,3].** However, Nb_2O_5 can only be activated under irradiation with UV light due to its wide band gap of approximately 3.1 eV, which makes its use of solar energy less efficient [**4,5].**

In this regard, many promising methods, including metallic and non-metallic doping, noble metal deposition or compositing with other semiconductors, have been developed to improve the efficiency of Nb_2O_5 as a photocatalytic material **[6,7]**.

Metal element doping has been proven to be one of the most effective approaches to extend the wide band gap semiconductor spectral response to the visible light region **[8].**

A literature survey shows that Nb_2O_5 nanofibers are frequently studied for their gas sensing or electrochemical properties, but little attention has been paid to their photocatalytic properties, in particular, there are no reports on the electrospinning fabrication and photocatalysis performance of Fe-doped Nb_2O_5 nanofibers.

In this study we are interested in the synthesis of the compound **Nb_2O_5-5%Fe** by high energy mechanical milling from Fe and Nb_2O_5 powders. These samples were characterized by X-ray diffraction.

General Introduction

The manuscript consists of a general introduction, a general conclusion and three chapters.

In the first chapter, we present a summary of the bibliographic study on the development of powder metallurgy, and high-energy mechanical milling mechanisms followed by general information on niobium pentoxide Nb_2O_5 covering its different properties and areas of use.

The second chapter describes the method for producing the **Nb_2O_5-5%Fe** compound and the experimental characterization techniques used in this study (XRD,).

The third chapter will summarize the results obtained during this study followed by a discussion which is in fact a necessary prerequisite for a good understanding of the phenomena occurring during the synthesis of these same materials.

Finally a general conclusion and the prospects for improvement of this material

References

[1] Rozina Abdul Rani, Ahmad Sabirin Zoolfakar, Anthony P. O'Mullane, Michael W. Austin and Kourosh Kalantar-Zadeh. Thin films and nanostructures of niobium pentoxide: fundamental properties, synthesis methods and applications. J.Mater.Chem.A, 2014, 2,15683

[2] H.Sch¨afer, R.GruehnandF.Schulte, Angew.Chem., Int.Ed. Engl.,1966,5,40–52.

[3] M.P.F.Graca, A.Meireles, C.NicoandM.A.Valente, J.Alloys Compd., 2013, 553,177–182.

[4] L.T.Arenas, P.C.M.Villis, J.Arguello, R.Landers,E.V.BenvenuttiandY.Gushikem,Talanta,2010,83,241 248.

[5] D.Velten, E.Eisenbarth, N.SchanneandJ.Breivie,J.Mater. Sci.:Mater.Med, 2004, 15,457–461.

[6] P.Griesmar, G.Papin, C.SanchezandJ.Livage, Chem. Mater., 1991, 3, 335–339.

[7] D. Rosenfeld, P. E. Schmid, S. Sz´eles, F. L´evy, V. Demarne and A. Grisel, Sens. Actuators, B, 1996, 37, 83–89.

[8]M.A.B.Gomes,L.O.d.S.Bulh˜oes,S.C.deCastroandJ.Dami˜ao,J.Electrochem.Soc.,1990,137, 3067–3070.

ChapterI: Mechanical Milling: Fundamentals and Applications

Chapter I :Mechanical Milling: Fundamentals and Applications

I- Mechanical Milling

1. Introduction

Powder processing is an important field in materials science because it allows the preparation of materials with controlled composition, fine particle size, and improved homogeneity. Compared with conventional methods, powder-based techniques are widely used for the synthesis of advanced materials such as ceramics, oxides, and composite systems.[1]

Among powder-processing methods, mechanical milling is considered an effective technique for modifying the structural properties of materials. During milling, the powder particles undergo repeated deformation, fracturing, and welding under mechanical energy, which leads to crystallite size reduction, lattice distortion, and defect formation.[2]

Mechanical milling is especially suitable for oxide materials and doping processes because it promotes a better distribution of dopant elements and improves solid-state interactions between powders. In the case of Nb_2O_5 doped with Fe, this technique can influence the structural and microstructural evolution of the material, which makes it highly relevant for the present study.[3]

2. Powder Metallurgy and Solid-State Processing

2.1 Definition of Powder Metallurgy

Powder metallurgy is a way to make things by using powders made of metal or ceramic to make parts or materials. There are a few steps in this process, such as getting the powders ready, mixing them, compacting them, and heating them. A lot of people use this method because it lets them have a lot of control over the composition and microstructure and avoids some of the problems that come up with traditional melting processes.[4]

2.2 Advantages of Powder Processing Techniques

There are many benefits to using powder processing methods in materials science. They let you make materials that are all the same and have a controlled chemical makeup, small particle size, and less material loss. These techniques can also be used to make materials that melt at high temperatures and to get refined or nanostructured microstructures after mechanical treatment[1]. People

also think that powder metallurgy is a cheap and flexible way to make advanced materials with certain properties.[4]

2.3 Applications in Advanced Materials

Advanced materials such as ceramics, oxide compounds, magnetic materials, structural alloys, and nanostructured systems are often made using powder metallurgy and solid-state processing. These techniques are particularly crucial for producing functional materials, as the ultimate characteristics are significantly influenced by composition, particle size, and structural uniformity[2]. Powder processing is especially useful for oxide materials because it makes it easier to mix, dope, and change the structure, which are all things that need to be done to make them work better.

3. Mechanical Milling

3.1 Definition and Historical Background

Mechanical milling is a powder processing technique based on the repeated fracturing, cold welding, and re-welding of powder particles under the action of mechanical energy. This method is widely used to produce fine, homogeneous, and structurally modified powders. It is considered an effective route for reducing particle size, increasing defect density, and improving the mixing of different powder components.

The development of mechanical milling is closely related to the work of J. S. Benjamin in the 1960s. His studies introduced the concept of mechanical alloying as a solid-state powder processing method capable of producing new materials through intensive milling. This contribution opened the way for the preparation of dispersion-strengthened materials and later for nanostructured and advanced engineering materials.

With the progress of milling equipment, **high-energy ball milling** was developed as an advanced technique capable of producing significant structural changes in powders within relatively short processing times. Compared with conventional milling, high-energy ball milling provides stronger impacts between balls and powder particles, leading to faster refinement, enhanced homogeneity, and possible phase transformations. For this reason, it has become an important method in the preparation and modification of metallic, ceramic, and oxide materials.

Figure 1 illustrates the mechanical milling process, where powder particles are subjected to repeated impact between milling balls, leading to deformation, fragmentation, and the formation of aggregates.

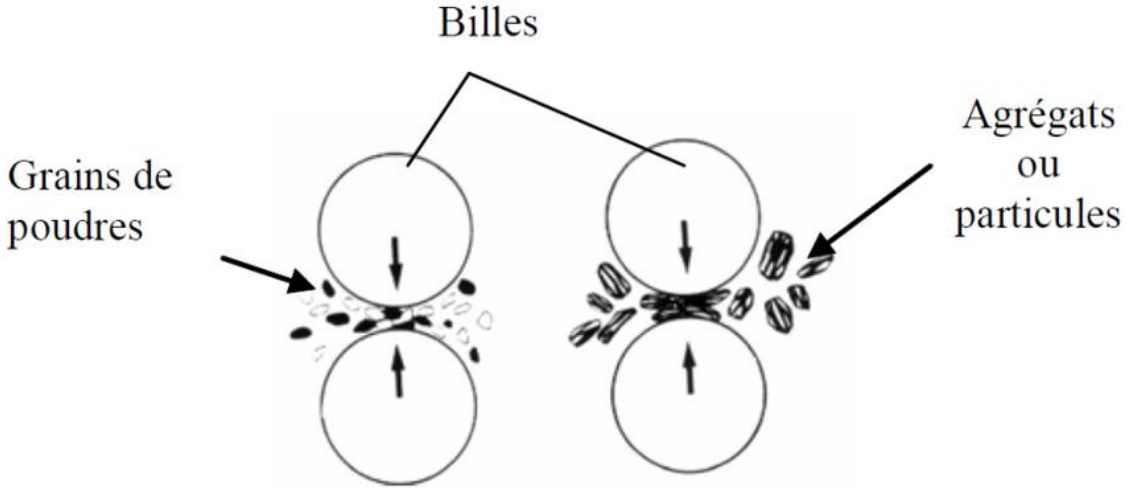

Figure 1 Schematic illustration of the mechanical milling process[5]

3.2 Types of Ball Mills

3.2.1 Planetary Ball Mill

The planetary ball mill is one of the most widely used devices in high-energy milling. Its operation is based on the rotation of the milling jar around its own axis while simultaneously revolving around a central axis. This combined motion generates strong impact and friction forces, which make the planetary mill highly effective for particle size reduction, structural refinement, and powder homogenization.[6]

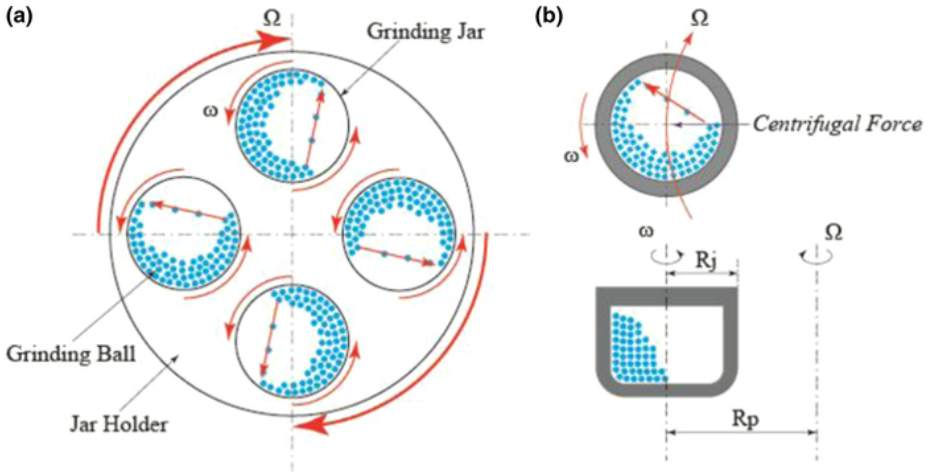

Figure 2 Schematic representation of a planetary ball mill[7]

This **figure 2** illustrates the operating principle of a planetary ball mill, where the grinding jars rotate around their own axes while revolving around a central axis, generating high-impact forces and effective powder refinement.

3.2.2 Vibratory Mill

The vibratory mill works by transmitting rapid oscillatory motion to the milling chamber, causing repeated collisions between the balls and the powder particles. Because of its high vibration frequency, this type of mill is considered suitable for fast milling and mechanical activation. It is often used when rapid refinement and repeated impacts are required.[8]

3.2.3 Attritor Mill

The attritor mill, also called a stirred ball mill, consists of a vertical or horizontal chamber containing grinding balls that are agitated by a rotating shaft with arms. This design allows efficient energy transfer and good powder mixing, making the attritor mill suitable for fine grinding and large-scale powder processing. It is widely used in mechanical alloying and advanced powder preparation.[9]

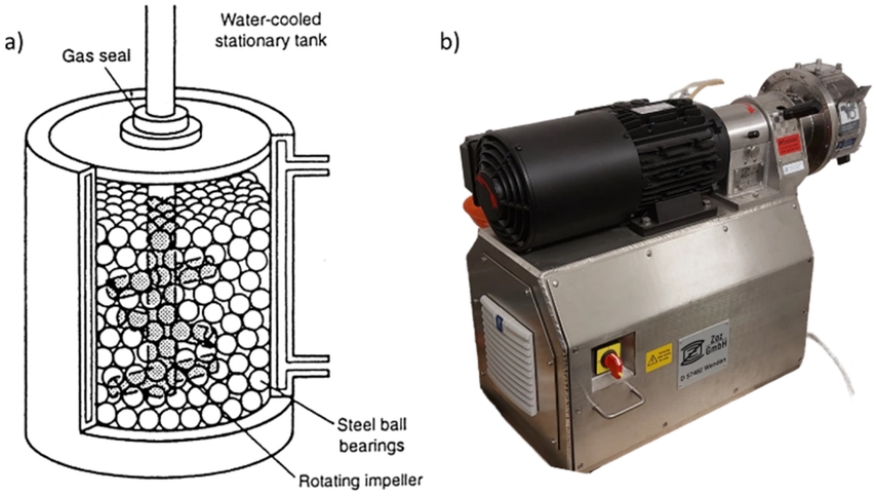

Figure 3 Schematic representation of an attritor mill.[10]

3.2.4 Conventional Ball Mill

The conventional ball mill is a rotating cylindrical device in which the powder is milled by the falling and rolling motion of the balls. Compared with high-energy mills, it provides lower milling energy and usually requires longer processing times. However, it remains widely used because of its simple design, low cost, and ease of operation.[1]

This **figure 4** shows the internal configuration of a conventional ball mill, where the rotation of the cylindrical chamber causes the grinding balls to crush and grind the powder material.

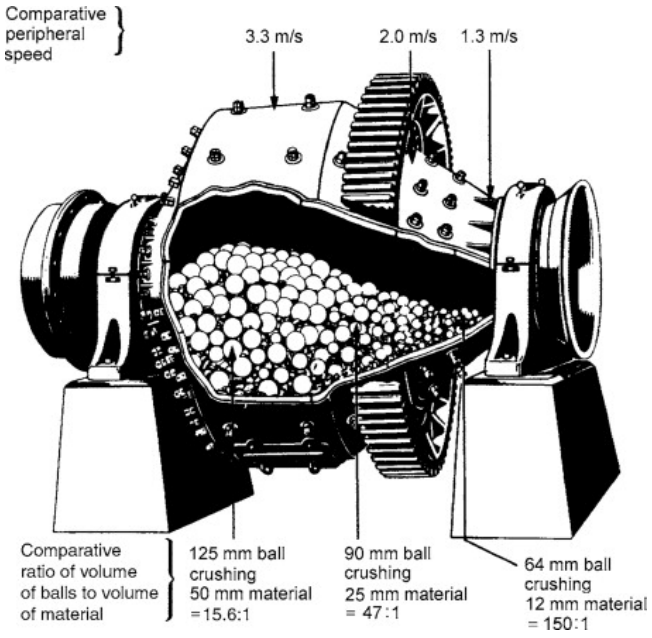

Figure 4 Schematic representation of a conventional ball mill[10]

3.3 Principle of Mechanical Milling

The principle of mechanical milling is based on the transfer of mechanical energy from the milling balls to the powder particles through repeated collisions during milling. These collisions generate high local pressures and temperatures for very short times, which cause important structural changes in the powder. As a result, mechanical milling is considered an effective top-down technique for particle refinement and microstructural modification (Suryanarayana, 2001; Yadav et al., 2012).

One of the main mechanisms involved in mechanical milling is the action of **impact forces**. During the rotation or vibration of the mill, the balls collide with the powder particles and with each other, producing compressive and shear forces. These forces are responsible for particle size reduction, defect formation, and increased internal strain in the material (Koch, 1993; Chaira & Karak, 2015).

Another important phenomenon is the competition between **fracturing and cold welding**. Brittle particles tend to fracture into smaller fragments under repeated impacts, whereas ductile particles may undergo plastic deformation and stick together, leading to cold welding. The balance between these two mechanisms controls the final particle size, morphology, and homogeneity of the milled powders.[11]

Mechanical milling also involves a **repeated deformation process** in which powder particles are continuously deformed, fractured, and rewelded. This cyclic process refines the structure, increases the density of defects, and may promote solid-state diffusion and phase transformation. Therefore, the structural evolution of the powder during milling strongly depends on the repetition of these deformation events.[12]

In the present study, this principle is particularly important because the repeated impacts during milling are expected to improve the distribution of Fe within the Nb_2O_5 matrix and to modify the structural and microstructural properties of the final powder.

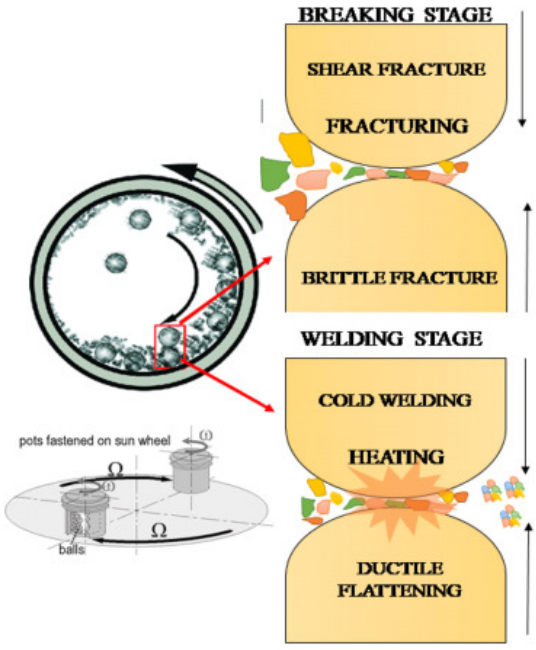

Figure 5 Schematic representation of the main stages occurring during mechanical milling, including fracturing, cold welding, and repeated deformation.[13]

This **figure 5** illustrates the main mechanisms involved in mechanical milling, including brittle fracture, ductile flattening, cold welding, and repeated deformation under the action of impact forces.

4. Mechanisms Occurring During Milling

4.1 Particle Size Reduction

Particle size reduction is one of the main mechanisms occurring during mechanical milling. It results from the repeated impact, compression, and shear forces generated by collisions between the milling balls and the powder particles. Under these conditions, the particles progressively break into smaller fragments, leading to a significant decrease in their average size.[14]

During the early stages of milling, large particles are subjected to intense mechanical stresses that cause fracture and fragmentation. As milling continues, the repeated collisions promote further refinement, although the rate of size reduction may decrease with time due to particle agglomeration or the balance between fracturing and cold welding.[8]

The reduction of particle size plays an important role in improving the surface area, homogeneity, and reactivity of the powder. In oxide systems, this mechanism may also contribute to structural refinement and enhanced diffusion between the constituent elements. Therefore, particle size reduction is considered a key factor in the evolution of the structural and microstructural properties of milled materials.[2]

In the present study, particle size reduction is expected to facilitate the dispersion of Fe in the Nb_2O_5 matrix and to promote better structural modification during milling.

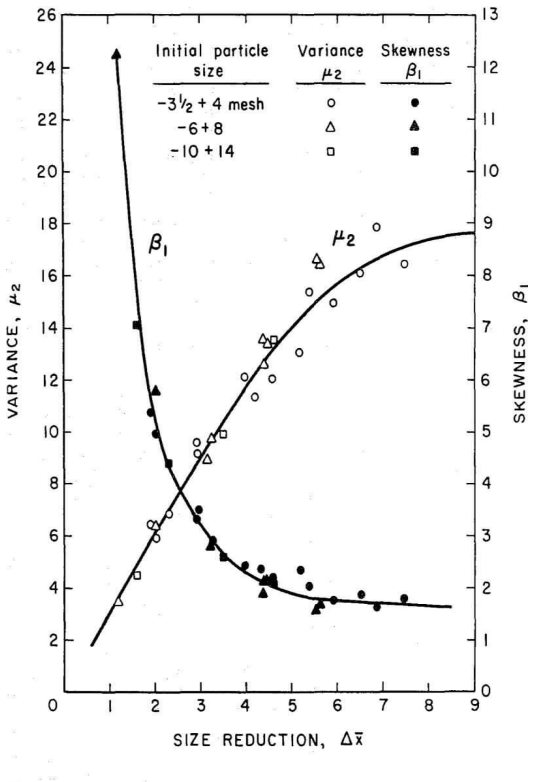

Figure 6 Evolution of particle size distribution parameters as a function of size reduction[15]

4.2 Structural Refinement

Structural refinement is one of the most important effects of mechanical milling. During the milling process, repeated impacts and severe plastic deformation progressively reduce the crystallite size and modify the internal structure of the material. This refinement is usually accompanied by an increase in lattice strain, defect density, and structural disorder.[2]

As milling time increases, the crystalline domains become smaller due to continuous deformation and fracture. At the same time, a large number of dislocations, vacancies, and grain boundaries are introduced into the structure. These defects contribute to the broadening of X-ray diffraction peaks and indicate the development of a refined and strained microstructure.[16]

Structural refinement is particularly important because it strongly affects the physical and chemical properties of the material. The reduction in crystallite size and the increase in structural defects may enhance diffusion, reactivity, and phase transformation during milling. In oxide materials, this mechanism can also modify the crystallinity and lattice organization of the host matrix.[17]

In the present study, structural refinement is expected to play a key role in the evolution of Nb_2O_5 after Fe addition and milling, especially through changes in crystallite size, lattice strain, and structural order.

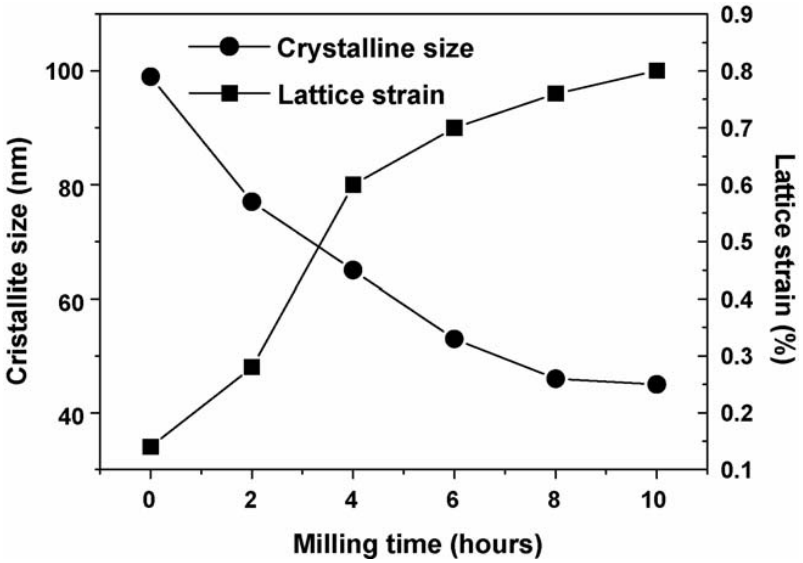

Figure 7 Evolution of crystallite size and lattice strain as a function of milling time[18]

Figure 7 shows that the crystallite size decreases with increasing milling time, whereas the lattice strain increases. This behavior indicates progressive structural refinement during mechanical milling. The reduction in crystallite size is mainly due to repeated fracturing and severe plastic deformation, while the increase in lattice strain is related to the accumulation of defects and distortions in the crystal lattice.

4.3 Formation of Solid Solutions

The formation of solid solutions is another important mechanism that may occur during mechanical milling. Under the repeated action of impact, fracturing, and cold welding, the powder particles are brought into very intimate contact, which enhances atomic diffusion at the interfaces. As a result, atoms of one element can gradually dissolve into the crystal lattice of another element, leading to the formation of a solid solution in the solid state.[19]

Mechanical milling is particularly effective for promoting solid-solution formation because it introduces a high density of defects such as dislocations, vacancies, and grain boundaries. These defects act as fast diffusion paths and accelerate atomic mixing even at relatively low temperatures. In many systems, this process may lead to the formation of metastable or supersaturated solid solutions that are difficult to obtain under equilibrium conditions.[16]

The formation of solid solutions during milling depends on several factors, including the nature of the constituent elements, milling intensity, milling time, and diffusivity of the species involved. In some cases, prolonged milling may produce a homogeneous distribution of the added element within the host matrix, which strongly influences the structural and functional properties of the final material.[8]

In the present study, the addition of Fe to Nb_2O_5 and the application of mechanical milling may enhance the dispersion of iron species in the oxide matrix and promote solid-state interactions that contribute to structural modification.

4.4 Phase Transformation

Phase transformation is another important phenomenon that may occur during mechanical milling. The repeated impacts generated during milling supply enough energy to disturb the initial crystal structure and, in some systems, to induce the formation of new phases. These transformations may involve the conversion of one crystalline phase into another, the formation of metastable phases, or even partial amorphization depending on the nature of the material and the milling conditions.[16]

The occurrence of phase transformation during milling is closely related to the continuous accumulation of defects, the reduction of crystallite size, and the increase in internal strain. These factors increase the stored energy of the material and may destabilize the original phase, making structural transformation more favorable. Therefore, prolonged milling can significantly modify the phase composition of the powders.[20]

In oxide materials, phase transformation may also be associated with the incorporation of dopant species and the progressive structural modification of the host lattice. For this reason, monitoring phase evolution is essential for understanding the effect of milling on the final properties of the material.

4.5 Defect Formation and Strain Accumulation

Mechanical milling is also characterized by the continuous formation of structural defects and the accumulation of internal strain. During repeated collisions, the powder particles undergo severe deformation, which introduces dislocations, vacancies, stacking faults, grain boundaries, and other imperfections into the crystal structure. These defects progressively accumulate as milling proceeds and strongly influence the structural state of the material.[2]

The accumulation of defects is generally accompanied by an increase in lattice strain. This strain results from distortions in the crystal lattice caused by the repeated mechanical stresses applied during milling. As the strain increases, the material becomes structurally less ordered, and X-ray diffraction peaks usually broaden, reflecting both defect formation and crystallite refinement.[16]

Defect formation and strain accumulation are important because they affect diffusion, phase stability, and microstructural evolution. In many cases, they also facilitate phase transformation and solid-solution formation by increasing the stored energy of the milled material. In the present study, these mechanisms are expected to contribute to the structural modification of Fe-added Nb_2O_5 during the milling process.

5. Parameters Affecting the Milling Process

The efficiency of the mechanical milling process strongly depends on several operating parameters. These parameters control the amount of energy transferred from the milling media to the powder particles and therefore influence particle size reduction, crystallite refinement, lattice strain, phase transformation, and powder homogeneity. Among the most important parameters are milling time, ball-to-powder weight ratio, milling speed, milling atmosphere, and the type and size of the milling balls.[21]

5.1 Milling Time

Milling time is one of the most influential parameters in mechanical milling. As milling time increases, powder particles are subjected to repeated collisions, which promote particle size reduction, crystallite refinement, and defect formation. In many cases, longer milling leads to a decrease in crystallite size and an increase in lattice strain due to the accumulation of structural disorder.[22]

However, excessive milling time may also produce undesirable effects such as powder agglomeration, contamination from the milling media, or excessive cold welding. Therefore, an optimum milling duration must be selected to obtain the desired structural modification without degrading the powder quality.

5.2 Ball-to-Powder Weight Ratio (BPR)

The ball-to-powder weight ratio (BPR) is defined as the ratio between the total mass of the milling balls and the mass of the powder charge. This parameter determines the frequency and intensity of impacts during milling. A higher BPR

generally increases the milling energy and improves particle refinement, homogenization, and reaction kinetics.[23]

On the other hand, an excessively high BPR may increase the temperature inside the vial and may also favor contamination or excessive cold welding. For this reason, the choice of BPR must be balanced according to the type of material, the mill used, and the desired final properties.

5.3 Milling Speed

Milling speed directly affects the kinetic energy of the balls and, consequently, the energy transferred to the powder particles. Increasing the milling speed usually increases the impact energy, which enhances particle breakage, structural refinement, and mixing efficiency. In high-energy mills, this parameter is particularly important because even small changes in speed may significantly modify the milling intensity.[24]

Nevertheless, very high milling speeds may produce excessive heating, increased wear of the vial and balls, and higher contamination levels. Therefore, milling speed should be optimized in order to achieve efficient grinding while maintaining good control over powder quality.[25]

5.4 Atmosphere (Air, Argon, Vacuum)

The milling atmosphere plays an important role in controlling chemical reactions during the milling process. Milling under air may promote oxidation, especially for reactive metallic powders, while inert atmospheres such as argon help minimize oxidation and contamination. Vacuum milling may also be used to limit undesired reactions with oxygen or moisture.[21]

The choice of atmosphere depends on the nature of the powder system. For oxide materials, air atmosphere may sometimes be acceptable, whereas metallic or highly reactive systems are often milled under argon or vacuum. Thus, atmosphere selection is essential for preserving the desired composition and ensuring the reproducibility of the process.[8]

5.5 Type and Size of Milling Balls

The type and size of milling balls strongly affect the energy transfer process. The material of the balls, such as steel, tungsten carbide, zirconia, or alumina, determines their hardness and density, which in turn influence impact energy and contamination risk. Harder and denser balls usually provide stronger

impacts, but they may also introduce impurities into the powder if wear occurs.[23]

Ball size is also a key factor. Larger balls generate stronger impact forces and are more effective for breaking coarse particles, whereas smaller balls provide a larger contact area and are better suited for fine grinding and homogenization. In practice, a combination of different ball sizes is often used to obtain both efficient fracture and good mixing of the powder.

Table 1 Main milling parameters and their effects

Parameter	Definition	Main effect on milling process
Milling time	Duration of the milling operation	Increases refinement, defect density, and structural changes
Ball-to-powder ratio (BPR)	Ratio of ball mass to powder mass	Controls impact frequency and milling energy
Milling speed	Rotation or vibration speed of the mill	Influences collision intensity and energy transfer
Atmosphere	Gas medium inside the vial	Controls oxidation, contamination, and chemical stability
Ball type and size	Material and diameter of the milling balls	Affects impact force, wear, contamination, and powder refinement

Table 2 General influence of milling parameters on powder characteristics

Parameter increase	Expected positive effect	Possible negative effect
Longer milling time	Smaller crystallite size, better homogeneity	Agglomeration, contamination, excessive cold welding
Higher BPR	Higher milling energy, faster refinement	Overheating, contamination, excessive deformation
Higher speed	Stronger impacts, faster particle breakage	Excessive heating, wear of balls and vial
Inert atmosphere	Reduced oxidation and better chemical control	More complex experimental setup
Larger balls	Stronger impact, faster fracture of coarse particles	Lower fine grinding efficiency
Smaller balls	Better homogenization and fine grinding	Lower impact energy for coarse particles

6. Advantages and Limitations of Mechanical Milling

Mechanical milling is widely used in materials science because it offers several important advantages for powder processing and structural modification. At the same time, this technique also presents some limitations that must be considered when selecting the experimental conditions. The balance between these advantages and limitations determines the effectiveness of the milling process and the quality of the final product.[2]

6.1 Advantages

One of the main advantages of mechanical milling is its ability to promote **nanostructure formation**. Under repeated impact and severe plastic deformation, the crystallite size can be reduced to the nanometer range, leading to refined microstructures and improved material properties. This ability makes mechanical milling an effective top-down route for producing nanocrystalline and nanostructured powders.[9]

Another important advantage is **homogeneous mixing**. During milling, repeated fracturing and rewelding ensure intimate contact between the different powder components, which improves chemical homogeneity and promotes a more uniform distribution of the added elements. This is especially useful in composite and doped systems where good dispersion of the second phase is required.

Mechanical milling also leads to **enhanced reactivity**. The reduction in particle size, increase in surface area, and introduction of defects raise the stored energy of the powder and facilitate solid-state reactions. As a result, milled powders often show improved diffusion behavior and higher chemical activity compared with unmilled materials.[20]

6.2 Limitations

Despite its advantages, mechanical milling has some important limitations. One of the major drawbacks is **contamination**. During prolonged milling, wear of the balls and vial may introduce foreign elements into the powder, especially when steel media are used. In addition, the milling atmosphere may also contribute to contamination if oxygen or moisture enters the vial.[2]

Another limitation is **agglomeration**. Fine powders produced by high-energy milling tend to stick together due to their high surface energy, which may reduce the efficiency of particle size reduction and affect powder homogeneity. Agglomeration is particularly common after long milling times and may complicate subsequent processing steps.[16]

Mechanical milling may also cause **excessive heating**. Repeated collisions generate heat inside the vial, and if this heat is not controlled, it may lead to undesirable effects such as phase instability, oxidation, or excessive cold welding. For this reason, milling is often performed in cycles with pauses in order to reduce temperature rise during processing.

7. Mechanical Milling of Oxide Materials

Mechanical milling is widely applied to oxide materials because it can induce important structural and microstructural modifications without requiring high processing temperatures. In oxide systems, repeated impacts during milling may reduce particle and crystallite size, increase defect density, modify phase composition, and improve the dispersion of added elements. These changes are particularly important because the properties of oxide materials strongly depend on their crystal structure, degree of order, and surface state.[26]

One of the main effects of milling on oxides is **structural modification**. The mechanical energy transferred during milling can distort the crystal lattice, generate disordered regions, and in some cases promote phase evolution or partial amorphization. In niobium pentoxide, this aspect is especially important because Nb_2O_5 is a polymorphic oxide whose properties are highly dependent on its structural form and crystallinity.[27]

A second important aspect is **grain refinement in** Nb_2O_5. During milling, repeated fracture and deformation progressively reduce the size of the crystalline domains, which leads to finer powders and a larger surface area. This grain refinement can strongly influence the reactivity and functional behavior of Nb_2O_5, especially when the oxide is combined with another element such as Fe. In oxide-based systems, smaller grains also facilitate a more homogeneous distribution of the added species in the host matrix.[28]

Mechanical milling also affects the **crystallinity** of oxide materials. In many cases, longer milling times lead to peak broadening in X-ray diffraction patterns, which indicates a reduction in crystallite size and an increase in structural disorder. For Nb_2O_5, changes in crystallinity are particularly significant because

they may alter the balance between ordered and disordered regions, thereby modifying the structural stability of the material. [29]However, the magnitude of this effect depends on the milling conditions, since some studies reported only limited crystallographic changes for Nb_2O_5 under specific processing conditions.

Another important consequence of milling is its **influence on optical properties**. In oxide materials, optical behavior is closely related to crystallite size, defect concentration, structural order, and electronic transitions. Since mechanical milling modifies these parameters, it may also affect the optical absorption behavior and the band gap of the material. In Nb_2O_5-based systems, optical properties are known to be sensitive to crystallinity and defect structure, which means that milling can play an important role in tuning the final optical response.[27]Therefore, studying the optical evolution of milled Nb_2O_5 is essential for understanding the effect of Fe addition in the present work.

In the present study, the mechanical milling of Nb_2O_5 with Fe is expected to promote structural refinement, modify the degree of crystallinity, and influence the optical behavior of the material through defect generation and better distribution of the added iron species.

Table 3 Main effects of mechanical milling on oxide materials

Effect	Description	Consequence
Structural modification	Lattice distortion and structural disorder	Changes in phase stability and crystal order
Grain refinement	Reduction in crystallite size	Higher surface area and improved dispersion
Change in crystallinity	Broadening of XRD peaks and reduced order	Modified structural and functional behavior
Optical modification	Defect and size-induced changes in absorption	Possible variation in band gap and optical response

Table 4 Relevance of milling effects for Nb_2O_5

Parameter	Effect of milling on Nb_2O_5	Importance for the present study
Crystal structure	May modify polymorphic stability and order	Important for XRD interpretation

Grain size	Decreases with continued milling	Affects microstructural evolution
Crystallinity	May decrease due to disorder and defects	Influences structural analysis
Optical properties	Sensitive to defects and structural changes	Important for UV–Visible study

II- Fundamental Properties

In the following section, an overview of the basic properties of Nb_2O_5 including crystal structure, electronic band diagram and electrical properties are presented. The fundamentals of the optical, mechanical and thermal properties of Nb_2O_5 are also discussed.

1. Crystal Structure

Niobium pentoxide ((Nb_2O_5) exhibits complex polymorphism. Depending on temperature and heat treatment, it exists in at least seven different crystal phases, all based on distorted arrangements of (NbO_6) octahedrons and some (NbO_7) or (NbO_4) polyhedra **[30].**

The three main structural phases of (Nb_2O_5) are:

- **TT phase** (**Low temperature / amorphous to pseudo-hexagonal**): Obtained by gentle heating (300 to 500 °C), this phase is characterized by a very disordered pseudo-hexagonal or monoclinic structure, with open tunnels facilitating ionic diffusion.
- **Phase T** (**Orthorhombic**): Forms at intermediate temperatures (600 to 900 °C). It has a more ordered structure based on octahedra linked by their vertices and edges.
- **Phase H or M** (**Monoclinic / High temperature**): Obtained above 900 °C until fusion. The H phase is the most thermodynamically stable and has a very complex structure containing blocks of NbO_6 octahedra.

Generally speaking, the Nb_2O_5 crystal lattice is characterized by Nb-O bonds forming complex layers, often interspersed with channels or tunnels along certain axes (notably the b axis) which give the material interesting properties for energy storage and catalysis **[31].**

Crystal structure Nb_2O_5 [2]
(Niobium in gray, oxygen in red)

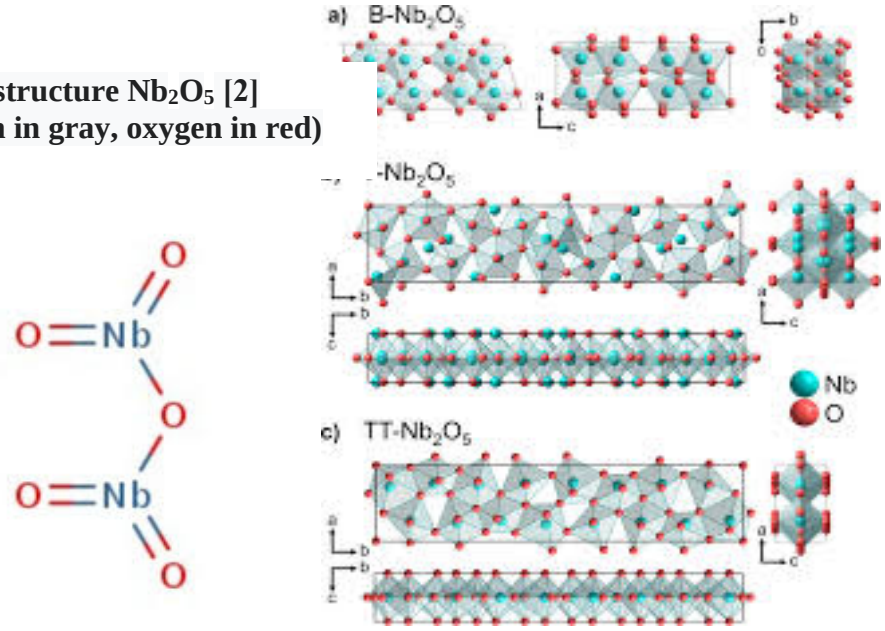

Properties	
Chemical formula	Nb_2O_5
Molar mass	265.81 g/mol
Appearance	White orthogonal solid
Density	4.06 g/cm^3
Melting point	1512 °C
Solubility in water	Insoluble
Solubility	Soluble in HF
Magnetic susceptibility (X)	-10.10^{-6} cm^3/mol

2. Band Energy Diagram And Electrical Properties[30]

In electronic device development based on metal oxides, several properties of the incorporated materials are of utmost importance. These include the band energy diagram, electrical conductivity and dielectric permittivity. Nb_2O_5 is a wide band gap n-type semiconductor with a conduction band comprised of empty Nb^{5+} 4d orbitals and has a conduction band value that is 0.2–0.4 eV higher than titanium dioxide (TiO_2) **[32].** Its band gap energy (E_g) values have been reported to be in the order of 3.1 (semiconducting) to 5.3 eV (insulating with conductivity of σ = 3 x 10^{-6} S cm^{-1}) **[33–34]**. The ability to tune the band

gap of Nb_2O_5 is possible and factors such as stoichiometry, crystallinity, heat treatment and incorporated foreign ions can dramatically influence the band gap energy. Previous studies have also shown that decreasing the dimensions of Nb_2O_5 into the nanoscale results in a blue shift of the energy gap, which can be attributed to the quantum-size effect **[35]**. Significantly, nanostructured Nb_2O_5 possesses grain dimensions that can critically influence the electronic structure of the material **[36].**

3. Optical Properties

As mentioned in Section II.2 the band gap of Nb_2O_5 ranges between 3.1 and 5.3 eV. As a result, Nb_2O_5, depending on its crystallinity and grain morphology can efficiently absorb light in the near UV and UV regions of the spectrum or it can be used as a transparent material to UV light. Nb_2O_5 has been identified as being capable of reversible and rapid coloration in the presence of intercalating ions such H^+ and Li^+ ions. It has been reported that this phenomenon can modulate the Nb_2O_5 optical transmission from a quasi-transparent state (T ~85%) to less than T ~ 10% in the ultraviolet (UV), visible or near infrared (IR) range, and can exhibit either a blue or brown colour depending on the crystallinity of the film **[37,38].**

The optical properties of Nb_2O_5 have been experimentally studied via various techniques such as spectrophotometry and spectroscopic ellipsometry [**39-42].**The refractive index value of Nb_2O_5 films has been reported to be in the order of 2 to 2.3 **[40,42].**Also the crystallinity of the film plays a significant contribution to the refractive index of the material as it decreases from 2.30 to 2.20 after being annealed from room temperature to 700 °C **[39].**

4. Mechanical Properties

Besides electronic and optical properties, an investigation of the mechanical properties of Nb_2O_5 is also of major importance for the fabrication of electronic devices especially for the development of flexible mechanical devices and

actuators such as micro electro-mechanical system (MEMS) devices. Stress or strain commonly occurs in thin films depending on the deposition process and constraints imposed by the substrate. The average hardness (H) and Young's modulus (E_r) values of as-sputtered Nb_2O_5films have been reported to be in the order of 5.6 to 6.8 GPa and 117 to 268 GPa respectively, which is again influenced by the crystal phase **[39,42].**

In flexible device applications, the bending test is essential to perform in order to monitor the effects of stretching on the device output and to make sure that all the component layers are stable even after several thousand flexes. Some of the appropriate flexibility tests and other related mechanical tests for electronic devices have been described in detail elsewhere **[43-46]**. Hota et al. have demonstrated that sputtered Nb_2O_5 thin films (~50 nm thickness) on flexible polyethylene terephthalate (PET) substrates show high mechanical flexibility in a repetitive bending test **[47]**.

5. Thermal properties

In an electronic system, heat dissipation is an acute problem due to miniaturization and the increasing power of microelectronic circuits. Thus, thermal conductor materials with high thermal conductivity and a low coefficient of thermal expansion (CTE) are essential for the purpose of heating and cooling. For Nb_2O_5, a limited number of studies have been carried out on its thermal properties. An investigation of the high-temperature thermal expansion of monoclinic Nb_2O_5 was conducted using X-ray and dilatometric techniques by Manning et al **[48]**. The results revealed that the lattice thermal expansion of Nb_2O_5 is anisotropic where the mean coefficients in the a, b, and c directions were 5.3 $x10^{-6}$, 0 and 5.9 x 10^{-6} per °C, respectively. Previous works also demonstrated the low thermal expansion behaviourof Nb_2O_5 over the temperature range of 20 to 1000 °C **[49, 50]**.

III. Applications

Applications of Nb_2O_5 normally involve the utilization of some unique properties of Nb_2O_5 such as its electronic and optical properties or biocompatibility which may be enhanced by the modification of Nb_2O_5films such that they significantly enhance the performance of a device. In the following sections, some of the most common applications of Nb_2O_5 that have been reported in the literature are presented.

1. Solar Cells and Light Emitting Diodes:

Nb_2O_5films are promising candidates for developing different types of optical devices, including solar cells based on dye-sensitized and heterojunction architectures as well as light emitting diodes (LEDs).

Since their discovery by Gratzel in 1991, dye sensitized solar cells (DSSCs) have been extensively studied as they offer the potential for clean, reliable, cost effective and on-site energy generation **[51]**. Increasing the efficiency of DSSCs depends on improving every single element in their structure, including: photoanode, dye, electrolyte and counter-electrode. However, the development of the most suitable photoanode will still have the most significant impact on the DSSCs's performance.

Nb_2O_5 has recently drawn considerable attention as a promising photoanode in view of its wider band gap (due to its higher conduction band edge) as well as comparable electron injection efficiency and better chemical stability in comparison to titanium oxide (TiO_2**) [53,53]**. These properties of Nb_2O_5 can potentially enhance the DSSCs' efficiency by increasing the open circuit voltage (V_{oc}) and photoconversion efficiency (η) **[54]**.

2. Sensing Devices:

Like other metal oxides such as TiO_2 and zinc oxide (ZnO), Nb_2O_5 has shown great potential to be used as a sensing material. Sensor devices based on Nb_2O_5 for gas, humidity, biological and chemical sensing as well as photodetection have been successfully demonstrated. Generally, the main parameters for good sensing device performance are the size, morphology, aspect ratio, intergranular

connectivity, porosity, surface energy, stoichiometry and surface area to volume ratio of the incorporated sensing material **[55,56]**.

3. Batteries and Supercapacitors :

The development of energy storage devices based on lithium ion batteries (LIBs) and supercapacitors have created great interest among researchers and Nb_2O_5 is certainly a favorable material for creating such storage devices **[57–60]**. Developing devices that can store sustainable energy with long term stability, very prolonged cycle life and meeting environmental constraints as well as safe operating potential windows (in the range of $1.0 \leq V \leq 3.0$ V vs. Li^+/Li) are the main goals of this field.

The study of Nb_2O_5 as an electrode material for lithium ion cells started in the early 1980s **[61, 62]**. The observations by Reichman et al. demonstrated that Nb_2O_5 can undergo intercalation with Li^+, leading to the possibility of repeated charging and discharging **[61]**. Subsequently, a LIB based on a Nb_2O_5 cathode was studied extensively by the Kumagai group **[63, 64, 65]**.

The structural changes of the Nb_2O_5 cathodes which are caused by discharging and recharging were investigated using X-ray photoelectron spectroscopy (XPS), X-ray diffraction (XRD) and

X-ray absorption fine structure (XAFS) analysis methods **[62,63]**. They suggested that tetragonal-Nb_2O_5 exhibited the best cycling performance with a large discharge capacity of 190 mA h g^{-1} for up to 30 cycles. XRD analysis suggested that the orthorhombic and tetragonal-Nb_2O_5 maintain their original crystal lattices, accompanying a small change in the cell volume even after Li^+ intercalation.

4. Catalysts:

Nb_2O_5 in its pure form has been used as a high temperature catalyst for the oxidative dehydrogenation (ODH) of organic materials in their gaseous form

such as methane to formaldehyde and propane to propene **[65, 66]**. In addition, other reports have demonstrated that Nb_2O_5 could serve as an efficient catalyst for the transesterification of β-keto esters with several kinds of alcohols, leading to good conversion at acceptable yields **[67]**. It has been suggested that the catalytic performance of each polymorphic form of Nb_2O_5 differs significantly from one another. However, Nb_2O_5 has commonly been used with other metal oxides/metals due to the following properties that it offers to the composite catalyst **[68-70]**: (i) promotion and support

properties: Nb_2O_5 enhances catalytic activity, selectivity and prolongs catalyst life when a small amount of this oxide is added to known catalysts, (ii) acidic property: the surface acid strength of hydrated Nb_2O_5 exhibits high catalytic activity, selectivity and stability for acid catalysed reactions in which water molecules participate, and (iii) redox properties and photosensitivity: Nb_2O_5 in mixed oxides is an oxidant and demonstrates photosensitivity.

5. Other Applications:

Nb_2O_5 has also been reported for applications other than those presented in Sections III.1 to III.5. As highlights, Nb_2O_5 has been incorporated in electronic devices such as memristors, capacitors, and field-effect transistors (FETs).

Highly crystalline orthorhombic Nb_2O_5 nanofibers obtained by electrospinning have been used in the development of memristors **[71]**.

Bibliography:

[1] C. Suryanarayana, « Mechanical alloying and milling », Prog. Mater. Sci., vol. 46, no 1, p. 1-184, janv. 2001, doi: 10.1016/S0079-6425(99)00010-9.

[2] C. C. Koch, « The synthesis and structure of nanocrystalline materials produced by mechanical attrition: A review », Nanostructured Mater., vol. 2, no 2, p. 109-129, mars 1993, doi: 10.1016/0965-9773(93)90016-5.

[3] M. S. El-Eskandarany, Mechanical Alloying: For Fabrication of Advanced Engineering Materials. Univ. Press of Mississippi, 2013.

[4] R. M. German, Powder Metallurgy Science. Metal Powder Industries Federation, 1994.

[5] J. Bran, « Elaboration and characterization of Cu-Co nanostructures: correlation with magneto-resistive properties », déc. 2012.

[6] « Modeling Planetary Ball Milling for Ceramics | PDF | Mill (Grinding) | Classical Mechanics », Scribd. Consulté le: 15 mars 2026. [En ligne]. Disponible sur: https://www.scribd.com/document/903578324/Modeling-of-the-Planetary-Ball-milling-Process-the-Case-Study-Of

[7] W. Gao, F. Chen, X. Wang, et Q. Meng, « Recent advances in processing food powders by using superfine grinding techniques: A review », Compr. Rev. Food Sci. Food Saf., vol. 19, juin 2020, doi: 10.1111/1541-4337.12580.

[8] B. Murty et S. Ranganathan, « Novel materials synthesis by mechanical alloying/milling », Int. Mater. Rev., vol. 43, p. 101-141, janv. 1998, doi: 10.1179/095066098790105654.

[9] D. Chaira, « Milling devices and mechanisms of mechanical alloying », 2024, p. 39-57. doi: 10.1016/B978-0-443-16151-3.00002-6.

[10] S. Triller, F. Winkelmann, J.-H. Schöbel, et M. Felderhoff, « Utilizing an attritor mill for solvent-free mechanochemical synthesis of rac-ibuprofen:nicotinamide co-crystals », RSC Mechanochemistry, vol. 2, p. 538-543, avr. 2025, doi: 10.1039/D5MR00020C.

[11] A. Nouri et C. Wen, « Surfactants in Mechanical Alloying/Milling: A Catch-22 Situation », vol. 39. 27 décembre 2013.

[12] C. Shuai et al., « Mechanical Alloying of Immiscible Metallic Systems: Process, Microstructure, and Mechanism », Adv. Eng. Mater., vol. 23, no 4, p. 2001098, 2021, doi: 10.1002/adem.202001098.

[13] R. Basu et A. Singh, « High temperature Si–Ge alloy towards thermoelectric applications: A comprehensive review », Mater. Today Phys., vol. 21, p. 100468, nov. 2021, doi: 10.1016/j.mtphys.2021.100468.

[14] D. L. Zhang, « Processing of advanced materials using high-energy mechanical milling », Prog. Mater. Sci., vol. 49, no 3, p. 537-560, janv. 2004, doi: 10.1016/S0079-6425(03)00034-3.

[15] « Particle Size Distribution of Grinding Mill Products - 911Metallurgist ». Consulté le: 16 mars 2026. [En ligne]. Disponible sur: https://www.911metallurgist.com/blog/particle-size-distribution-grinding-mill-products/

[16] M. H. Enayati et F. A. Mohamed, « Application of mechanical alloying/milling for synthesis of nanocrystalline and amorphous materials », Int. Mater. Rev., vol. 59, no 7, p. 394-416, sept. 2014, doi: 10.1179/1743280414Y.0000000036.

[17] G. Rajender et P. K. Giri, « Strain induced phase formation, microstructural evolution and bandgap narrowing in strained TiO2 nanocrystals grown by ball milling », J. Alloys Compd., vol. 676, p. 591-600, août 2016, doi: 10.1016/j.jallcom.2016.03.154.

[18] J. Fogagnolo, D. Amador, E. Ruiz-Navas, et J. Torralba, « Solid solution in Al–4.5wt% Cu produced by mechanical alloying », Mater. Sci. Eng. A, vol. 433, p. 45-49, oct. 2006, doi: 10.1016/j.msea.2006.07.005.
[19] L. Lu et M. O. Lai, « Formation of new materials in the solid state by mechanical alloying », Mater. Des., vol. 16, no 1, p. 33-39, janv. 1995, doi: 10.1016/0261-3069(95)00005-J.
[20] T. P. Yadav, R. M. Yadav, et D. P. Singh, « Mechanical Milling: a Top Down Approach for the Synthesis of Nanomaterials and Nanocomposites », Nanosci. Nanotechnol., vol. 2, no 3, p. 22-48, 2012.
[21] F. Hadef et A. Otmani, « Mechanical Alloying/Milling », in Handbook of Mechanical Nanostructuring, 1re éd., M. Aliofkhazraei, Éd., Wiley, 2015, p. 263-276. doi: 10.1002/9783527674947.ch12.
[22] M. Toozandehjani, K. A. Matori, F. Ostovan, S. Abdul Aziz, et M. S. Mamat, « Effect of Milling Time on the Microstructure, Physical and Mechanical Properties of Al-Al2O3 Nanocomposite Synthesized by Ball Milling and Powder Metallurgy », Materials, vol. 10, no 11, p. 1232, nov. 2017, doi: 10.3390/ma10111232.
[23] C. F. Burmeister et A. Kwade, « Process engineering with planetary ball mills », Chem. Soc. Rev., vol. 42, no 18, p. 7660-7667, août 2013, doi: 10.1039/C3CS35455E.
[24] F. J. Gotor, M. Achimovicova, C. Real, et P. Balaz, « Influence of the milling parameters on the mechanical work intensity in planetary mills », Powder Technol., vol. 233, p. 1-7, janv. 2013, doi: 10.1016/j.powtec.2012.08.031.
[25] R. S. Maurya, « Effect of Milling Parameters and Milling Energy on Amorphization: A Review », Trans. Indian Inst. Met., 2023, doi: 10.1007/s12666-023-02929-x.
[26] J. Koruza, T. Rojac, et B. Malič, « Polar Oxide Nanopowders Prepared by Mechanical Treatments », in Handbook of Mechanical Nanostructuring, John Wiley & Sons, Ltd, 2015, p. 641-661. doi: 10.1002/9783527674947.ch27.
[27] R. Pang, Z. Wang, J. Li, et K. Chen, « Polymorphs of Nb2O5 Compound and Their Electrical Energy Storage Applications », Materials, vol. 16, no 21, p. 6956, janv. 2023, doi: 10.3390/ma16216956.
[28] A. K. Kushwaha, M. John, M. Misra, et P. L. Menezes, « Nanocrystalline Materials: Synthesis, Characterization, Properties, and Applications », Crystals, vol. 11, no 11, p. 1317, nov. 2021, doi: 10.3390/cryst11111317.
[29] M. R. N. Soares et al., « Effect of processing method on physical properties of Nb2O5 », J. Eur. Ceram. Soc., vol. 31, p. 501, avr. 2011, doi: 10.1016/j.jeurceramsoc.2010.10.024.
[30] M.P.F. Graca, A. Meireles, C. Nico and M.A. Valente, J. Alloys Compd., 2013, 553, 177–182.
[31] G. R. Lee and J. A. Crayston, J. Mater. Chem., 1991, 1, 381–386.
[32] M.A. Aegerter, M. Schmitt and Y.P. Guo, Int. J. Photoenergy, 2002, 4, 1–10.
[33] D. Co¸skun and S. Demirela, Appl. Surf. Sci., 2013, 277, 35–39.
[34] K. Kamada, M. Mukai and Y. Matsumoto, Electrochim. Acta, 2004, 49, 321–327.
[35] S. Abe, Nanoscale Res. Lett., 2012, 7, 1–6.
[36] G. Brauer, Z. Anorg. Allg. Chem., 1941, 248, 1–31.
[37] Rozina Abdul Rani, Ahmad Sabirin Zoolfakar, Anthony P. O'Mullane, Michael W. Austin and Kourosh Kalantar-Zadeh. Thin films and nanostructures of niobium pentoxide: fundamental properties, synthesis methods and applications. J. Mater. Chem. A, 2014, 2, 15683.
[38] Gustavo Henrique M. Gomes, Nelcy D.S. Mohallem. Materials Letters, Volume 318, 1 July 2022, 132136.

[39] H. Luo, W. Song, P. G. Hoertz, K. Hanson, R. Ghosh, S. Rangan, M. K. Brennaman, J. J. Concepcion, R. A. Binstead, R. A. Bartynski, R. Lopez and T. J. Meyer, Chem. Mater., 2012, 25, 122–131.
[40] J. W. Schultze and M. M. Lohrengel, Electrochim. Acta, 2000, 45, 2499–2513.
[41] T. Proslier, J. Zasadzinski, L. Cooley, M. Pellin, J. Norem, J. Elam, C. Z. Antoine, R. A. Rimmer and P. Kneisel, IEEE Trans. Appl. Supercond., 2009, 19, 1404–1408.
[42] S. Zhuiykov and E. Kats, World Academy of Science, Engineering and Technology, 2013, vol. 78.
[43] A. D. Yoffe, Adv. Phys., 2002, 51, 799–890.
[44] K. Sattler, The energy gap of clusters, nanoparticles, and quantum dots, Academic Press, New York, 2002.
[45] M. A. Aegerter, M. Schmitt and Y. P. Guo, Int. J. Photoenergy, 2002, 4, 1–10.
[46] A. Pawlicka, M. Atik and M. A. Aegerter, Thin Solid Films, 1997, 301, 236–241.
[47] E. Çetin¨org¨u-Goldenberg, J.-E. Klemberg-Sapieha and L. Martinu, Appl. Opt., 2012, 51, 6498–6507.
[48] C.-C. Lee, C.-L. Tien and J.-C. Hsu, Appl. Opt., 2002, 41, 2043–2047.
[49] N. ¨Ozer, M. D. Rubin and C. M. Lampert, Sol. Energy Mater. Sol. Cells, 1996, 40, 285–296.
[50] X. Xiao, G. Dong, C. Xu, H. He, H. Qi, Z. Fan and J. Shao, Appl. Surf. Sci., 2008, 255, 2192–2195.
[51] S. Park, G. Wang, B. Cho, Y. Kim, S. Song, Y. Ji, M.-H. Yoon and T. Lee, Nat. Nano, 2012, 7, 438–442.
[52] J. Lewis, Mater. Today, 2006, 9, 38–45.
[53] J. Hu, L. Li, H. Lin, P. Zhang, W. Zhou and Z. Ma, Opt. Mater. Express, 2013, 3, 1313–1331.
[54] C. Peng, Z. Jia, H. Neilson, T. Li and J. Lou, Adv. Eng. Mater., 2013, 15, 250–256.
[55] M. K. Hota, M. K. Bera and C. K. Maiti, Semicond. Sci. Technol., 2012, 27, 105001.
[56] W. R. Manning, O. Hunter, F. W. Calderwood and D. W. Stacy, J. Am. Ceram. Soc., 1972, 55, 342–347.
[57] D. L. Douglass, J. Less-Common Met., 1963, 5, 151–157.
[58] G. L. Dwivedi and E. C. Subbarao, J. Am. Ceram. Soc., 1973, 56, 443–444.
[59] G. Michael, J. Photochem. Photobiol., C, 2003, 4, 145–153.
[60] J. Z. Ou, R. A. Rani, M. H. Ham, M. R. Field, Y. Zhang, H. Zheng, P. Reece, S. Zhuiykov, S. Sriram, M. Bhaskaran, R. B. Kaner and K. Kalantar-Zadeh, ACS Nano, 2012, 6, 4045–4053.
[61] L. Alibabaei, H. Luo, R. L. House, P. G. Hoertz, R. Lopez and T. J. Meyer, J. Mater. Chem. A, 2013, 1, 4133–4145.
[62] R. Jose, V. Thavasi and S. Ramakrishna, J. Am. Ceram. Soc., 2009, 92, 289–301.
[63] G. Shen, P.-C. Chen, K. Ryu and C. Zhou, J. Mater. Chem., 2009, 19, 828–839.
[64] N. S. Harale, D. L. Kamble, M. G. Gang, V. K. Rao, J. H. Kim and P. S. Patil, Mater. Today, 2013, 16, 452–453.
[65] V. Etacheri, R. Marom, R. Elazari, G. Salitra and D. Aurbach, Energy Environ. Sci., 2011, 4, 3243–3262.
[66] M. V. Reddy, G. V. Subba Rao and B. V. R. Chowdari, Chem. Rev., 2013, 113, 5364–5457.
[67] K. Naoi, S. Ishimoto, J.-i. Miyamoto and W. Naoi, Energy Environ. Sci., 2012, 5, 9363–9373.
[68] Y. Jing, Z. Zhou, C. R. Cabrera and Z. Chen, J. Mater. Chem. A, 2014, 2, 12104–12122.
[69] B. Reichman and A. J. Bard, J. Electrochem. Soc., 1981, 128, 344–346.

[70] N. Kumagai, K. Tanno, T. Nakajima and N. Watanabe, Electrochim. Acta, 1983, 28, 17–22.
[71] R. Kodama, Y. Terada, I. Nakai, S. Komaba and N. Kumagai, J. Electrochem. Soc., 2006, 153, A583–A588.

ChapterII :Experimental Procedures

Chapter II: Experimental Procedures

1. Introduction

This chapter presents the experimental methodology adopted for the preparation of Fe-doped niobium pentoxide (Nb_2O_5–5%Fe) powders using the mechanical milling technique. It also describes the characterization methods employed to investigate the structural and microstructural changes induced by iron addition and milling time.

The purpose of this study is to evaluate the effect of 5% Fe incorporation on the evolution of the structural and microstructural properties of Nb_2O_5, with particular attention to phase composition, crystallite size, and optical behavior. The characterization of the synthesized powders was carried out using X-ray Diffraction (XRD) and UV-Visible spectroscopy.

2. Preparation of Samples

2.1. Characteristics of Starting Materials

High-purity niobium pentoxide (Nb_2O_5) and iron (Fe) powders were used as starting materials for the preparation of Nb_2O_5–5%Fe composite powders. The powders were used without further purification.

The main characteristics of the starting powders are summarized in Table II.1.

Table 5 Characteristics of the starting powders

Element	Particle Size	Purity (%)	Form	Supplier / Characteristics
Nb_2O_5	< 45 µm	99.9	Powder	Commercial grade
Fe	< 45 µm	99.8	Powder	Commercial grade

2.2. Weighing of Powders

For the preparation of Nb_2O_5–5%Fe composite powders, a total mass of 5 g was selected for each sample. The required amounts of niobium pentoxide (Nb_2O_5) and iron (Fe) powders were calculated according to the nominal composition of 5 wt.% Fe added to Nb_2O_5.

The masses were determined using the following relation:

$$Nb_2O_5\ (95\ wt.\ \%) + Fe\ (5\ wt.\ \%) \rightarrow Nb_2O_5\text{–}5\%Fe$$

The powders were weighed with an accuracy of 10^{-4} g using a high-precision electronic balance (OHAUS Traveler). Accurate weighing ensures proper composition control and reproducibility of the experimental results.

Figure 8balance

2.3. Mixing and Mechanical Milling

The weighed powders were mixed and homogenized using a high-energy vibratory ball mill. The milling process promotes intimate mixing between Nb_2O_5 and Fe particles and enhances solid-state diffusion during prolonged milling.

The principle of the vibratory mill consists of subjecting the powder mixture and milling balls to high-frequency oscillatory motion in three perpendicular directions. This movement generates repeated impacts and shear forces that reduce particle size and improve homogeneity.

The milling process was carried out at different durations: **1 h, 3 h, 6 h, 12 h, and 24 h**.

To avoid excessive heating, milling was performed in cycles of 30 minutes with intermediate pauses when necessary. This procedure ensures uniform mixing and controlled microstructural evolution.

2.4. Pellet Formation

The powder compaction process ensures good particle-to-particle contact, reduces porosity, and improves the mechanical stability of the samples prior to characterization. This step plays an important role in obtaining dense and homogeneous pellets suitable for structural and optical measurements.

In the present study, 5 g of Nb_2O_5–5 wt. % Fe powder mixture was compacted at room temperature using a uniaxial pressing technique. The compaction was carried

out using a Specac laboratory pellet press (Model GS25011) with a maximum capacity of 25 tons.

The powder was first placed into a cylindrical stainless-steel die (Figure II.2). A uniaxial load of 10 tons was then applied for 5 minutes using the upper punch to ensure proper densification.

The obtained samples were cylindrical pellets with a diameter of 20 mm and an approximate thickness of 2 mm.

Figure 9 Hydraulic press used for pellet preparation

Figure 10 Cylindrical pellets obtained after uniaxial pressing

2.6. Surface Preparation

Polishing is a surface preparation process intended to obtain a smooth and scratch-free surface prior to microscopic examination. The procedure involves grinding the sample surface using silicon carbide abrasive papers of progressively finer grit sizes.

During polishing, the sample is rotated by 90° every minute to ensure uniform material removal. The abrasive papers are mounted on a rotating polishing disc and continuously cooled with water to minimize overheating and reduce paper wear.

The polishing operation was carried out using a MECAPOL P 230 manual polishing machine with a rotating disc diameter of 200–250 mm and adjustable speed ranging from 20 to 600 rpm.

Figure 11 Manual polishing machine used for sample preparation

3. Characterization Techniques

For a better understanding of the structural properties of the synthesized Nb_2O_5–5 wt. % Fe powders, the following characterization techniques were employed: X-ray diffraction (XRD).

3.1. Structural Study by X-ray Diffraction (XRD)

X-rays are electromagnetic radiations with wavelengths on the order of angstroms (Å), which are comparable to the interatomic distances in crystalline materials. This makes X-ray diffraction a powerful tool for investigating crystal structure, phase composition, and microstructural evolution.

The XRD analysis of the milled Nb_2O_5–5 wt. % Fe samples was performed using a Bruker D8 Advance diffractometer (Figure 14). The measurements were carried out using Cu Kα radiation with a wavelength $\lambda = 1.5406$ Å.

The diffraction patterns were recorded over an appropriate 2θ range in order to identify the crystalline phases present and to study the effect of Fe addition and milling time on the structural properties of Nb_2O_5.

Figure 12 : Bruker D8 Advance X-ray diffractometer used for structural analysis

3.1.1. Principle of X-ray Diffraction

X-ray diffraction is a simple, non-destructive technique widely used for microstructural characterization of crystalline materials in powder form.

When a monochromatic X-ray beam strikes a crystalline material at an incident angle θ, the X-rays are scattered by the electrons of the atoms. Constructive interference occurs only when the scattered waves satisfy Bragg's condition, producing detectable diffraction peaks.

The condition for diffraction is given by Bragg's law:

$$2\, d \sin\theta = n\, \lambda$$

where:
θ is the Bragg angle,
n is the diffraction order,
λ is the wavelength of the incident X-rays,
d is the interplanar spacing,
(hkl) are the Miller indices of the crystallographic planes.

This relationship allows determination of the lattice parameters, crystallite size, and structural modifications induced by Fe incorporation and mechanical milling.

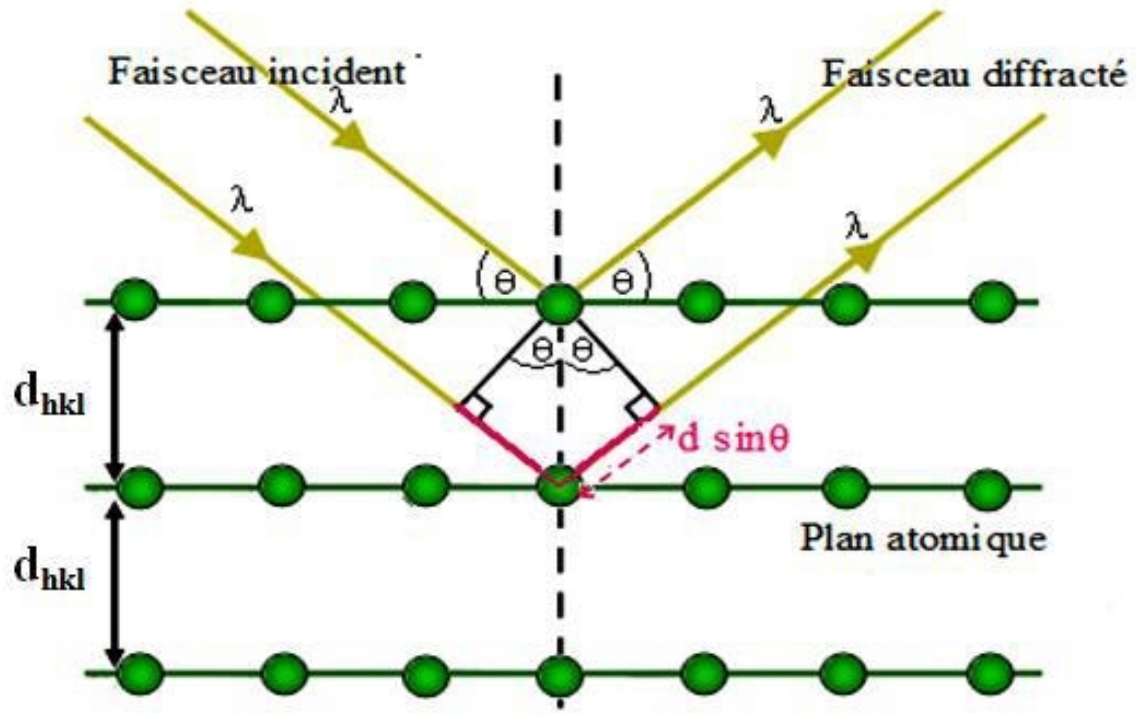

Figure 13 : Schematic representation of X-ray diffraction by a crystalline lattice

ChapterIII: Results and Discussion

Chapter III: Results and Discussion

1. Introduction

This chapter is mainly devoted to the study of the structural and microstructural evolution of Nb_2O_5–5% Fe compounds prepared by high-energy mechanical milling as a function of milling time, t, from 01 to 24 h. The different phases formed were analyzed by X-ray diffraction (XRD).

Data processing, phase identification, and Rietveld refinement, used to accurately fit the diffraction peak profiles of Nb_2O_5–5% Fe powders produced by high-energy mechanical milling as a function of milling time, t, from 01 to 24 h, were carried out using X'PertHighScore software. This software contains a database corresponding to the JCPDS cards of various existing materials. Post-processing, detailed peak analysis and the creation of high-quality graphs were performed using Origin Pro software.

The calculation of microstrains and dislocation density was performed using the Williamson–Hall (W–H) method [1].

Microstrain is deduced from the slope of the Williamson–Hall plot, where β cosθ is plotted as a function of 4 sinθ.

$$\boldsymbol{\beta^{hkl} . Cos\theta} = \frac{\boldsymbol{K}}{\boldsymbol{D}} + 4 . \boldsymbol{\varepsilon} . \boldsymbol{Sin\theta}$$

λ= x-ray wavelength

D = average crystallite size

K = shape factor (typically equal to = 0,9)

Dislocation density formula $\boldsymbol{\delta} = \frac{1}{\boldsymbol{D^2}}$

The dislocation density, denoted δ, represents the length of dislocations per unit volume (m/m³ or m^{-2}). Based on the sizes of the crystallites (nanomaterials):

$$\boldsymbol{\delta} = \frac{1}{\boldsymbol{D^2}}$$

D = average crystallite size in **(nm)**

δ = dislocation density $(\boldsymbol{m^{-2}})$

2. X-ray Diffraction Analysis

The main objective of this study is to follow the structural and microstructural evolution of the Nb_2O_5 system doped with 5% iron, prepared by high-energy mechanosynthesis. This process produces profound transformations within the crystal lattice during 24 hours of treatment.

The diffractogram in Figure 14 presents the results of the X-ray diffraction analysis performed on the reference sample Nb_2O_5–5% Fe without milling (00 h of milling).

The spectrum shows the coexistence of two phases: Nb_2O_5 and Fe. The diffraction peaks located at 16.9°, 22.6°, 28.4°, 28.9°, 36.6°, 46.1°, 50.0°, 50.9°, 55.4°, 56.4°, and 58.8° can be indexed, respectively, to the (130), (001), (180), (200), (181), (002), (1160), (380), (182), (381), and (2161) planes of an orthorhombic Nb_2O_5 structure (JCPDS card No. 00-027-1313), with lattice parameters a = 6.1680 Å, b = 29.3120 Å, c = 3.9380 Å, and α = β = γ = 90.00°.

The peak located at 46.6° belongs to the (011) plane of iron (Fe), which has a cubic structure with lattice parameters a = b = c = 2.8670 Å and α = β = γ = 90.00° (JCPDS card No. 96-411-3937).

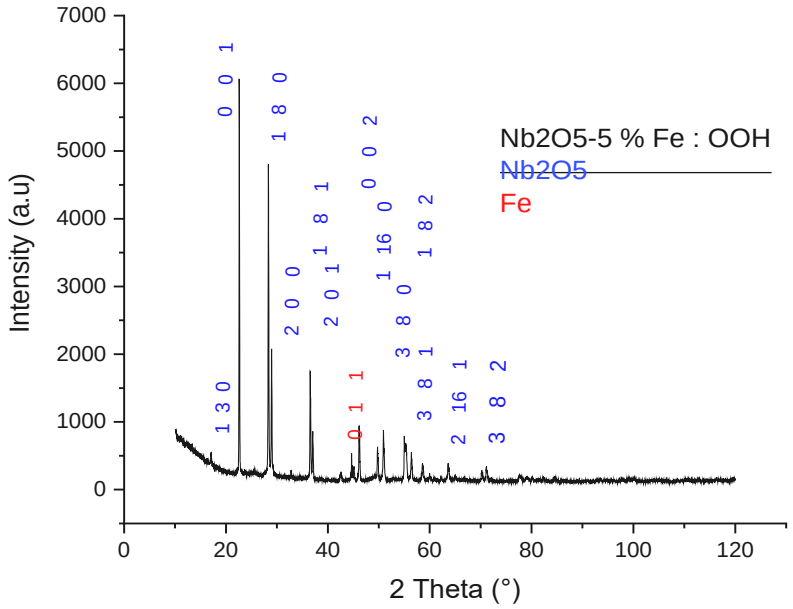

Figure 14 : Diffraction pattern of an unmilled Nb_2O_5–5% Fe sample

The diffraction patterns of the samples milled from 01 h to 24 h are shown in Figure 14.

According to the results shown in the figure, milling induces significant and progressive changes in the crystalline structure of the samples as a function of milling time.

At 0 h, that is, before the beginning of the milling process, the diffraction patterns reveal the presence of all characteristic peaks of niobium pentoxide Nb_2O_5 and iron Fe, as shown above. These initial results indicate that, before milling, the two elements exist in distinct and well-defined crystalline forms.

Peak indexing, a crucial step for the correct interpretation of diffraction patterns, was carried out using X'PertHighScore software. This software includes a comprehensive database containing JCPDS cards for various existing materials. JCPDS cards (Joint Committee on Powder Diffraction Standards) are internationally recognized references for the identification of crystalline phases from X-ray diffraction data. Using this database, the diffraction peaks were accurately identified and assigned to the corresponding positions of the niobium oxide and iron phases present in the samples.

After 1, 3, 6, 12, and 24 hours of milling, it was observed that the X-ray diffraction patterns of all samples have similar shapes. However, they differ in peak intensity and angular position. Moreover, after 3 h of milling, the complete disappearance of the iron peaks was observed for all studied samples, together with the formation of a new phase attributed to $FeNb_2O_6$ (iron niobium oxide), which has a tetragonal structure with lattice parameters a = b = 4.7270 Å, c = 9.2160 Å, and $\alpha = \beta = \gamma = 90.00°$ (JCPDS card No. 01-077-1290).

Figure 15 shows the X-ray diffraction (XRD) patterns of Nb_2O_5-5wt.%Fe powders milled from 01h to 24h . the figure illustrates the evolution of the diffraction peaks with increasing milling time.

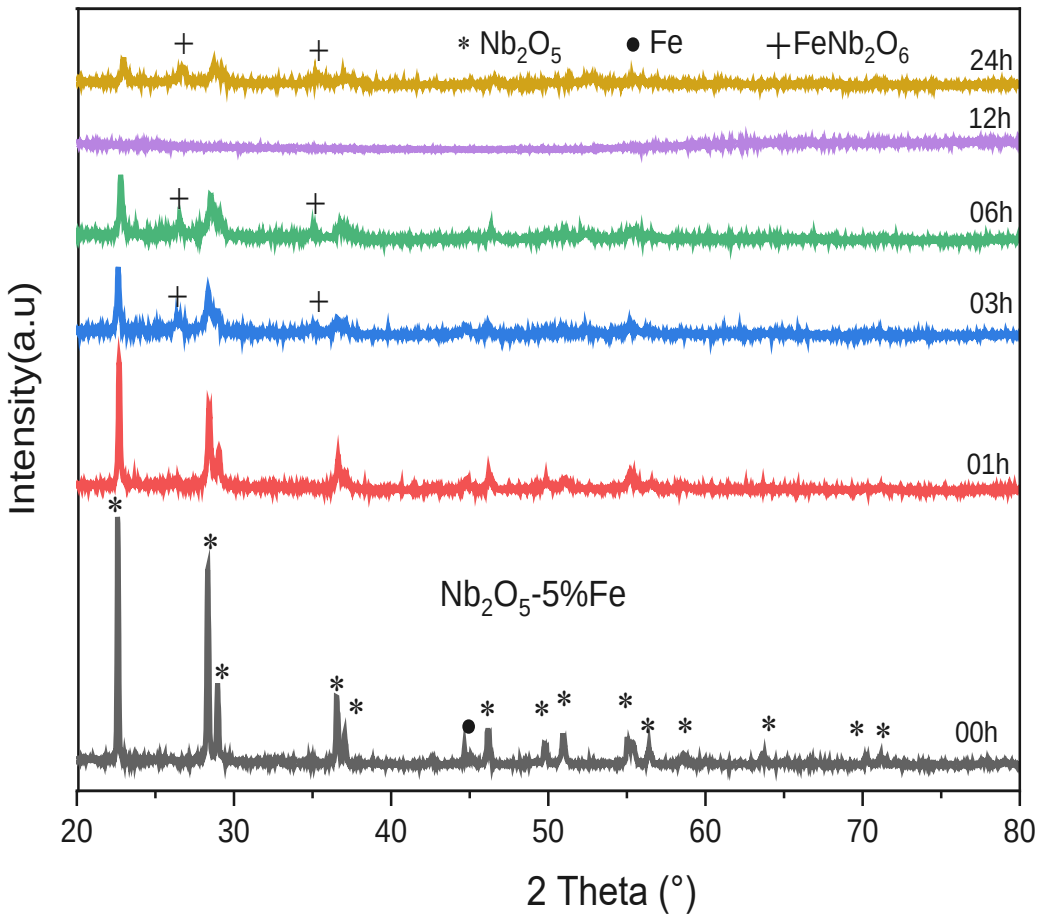

Figure 15 : Diffraction patterns of Nb_2O_5–5% Fe samples milled from 0 to 24 h

The orthorhombic structure of Nb_2O_5 remains stable. No diffraction peak corresponding to separated iron oxides, such as Fe_2O_3, is generally detected at this 5% doping level.

The complete disappearance of the iron peaks was accompanied by a shift toward higher angles, as shown in Figures 18, 19. This angular shift is clearly visible in the X-ray diffraction patterns and provides strong evidence that iron atoms have dissolved into the Nb_2O_5 crystal lattice. In particular, at a concentration of 5%, iron generally enters the crystal lattice by substituting Nb^{5+} ions because of the similarity in ionic size.

This shift toward higher angles, meaning an increase in 2θ, indicates a contraction of the crystal lattice. Since Fe^{3+} is slightly smaller or may create oxygen vacancies (V_O) that tighten the structure, the atomic planes move closer together.

The incorporation of iron into the niobium oxide structure causes significant changes in the crystal lattice. When iron atoms enter the Nb_2O_5 lattice, they modify the interplanar distances, that is, the distances between successive atomic planes in the crystal, as shown in Table 6. This incorporation modifies the lattice parameters and appears as a shift of the diffraction peaks toward higher angles. Although the ionic radius of Fe^{3+} (0.64 Å) is close to that of Nb^{5+} (approximately 0.64 Å), the difference in valence (+3 compared with +5) creates local stresses that often lead to contraction or expansion of the lattice parameters (a, b, c), resulting in lattice distortion.

The results shown in Table 6 clearly indicate changes in the interplanar distances of the most intense peaks, with a contraction trend mainly caused by milling at different times.

Thus, unlike conventional thermal substitutional doping, which often expands the lattice, mechanical milling with 5% Fe appears to cause lattice compression. This can be explained by the forced insertion of iron into interstitial sites or by a reduction in interatomic distances due to the high local pressures generated during ball impacts.

Table 6 Variation of the interplanar distances d_{hkl} of the most intense peaks as a function of milling time

Plane (h k l)	d (Å) at 00 h	d (Å) at 01 h	d (Å) at 03 h	d (Å) at 06 h	d (Å) at 24 h	Trend
(0 0 1)	3.93174	3.91782	3.92869	3.90339	3.86478	Strong contraction
(1 8 0)	3.14897	3.14068	3.14383	3.12851	3.10844	Contraction
(2 0 0)	3.08225	3.07222	3.07734	3.0614	3.04392	Contraction

The angular shift of the diffraction peaks observed in the spectra may also be attributed to first-order internal stresses, or microdistortions, induced by the milling process. These internal stresses result from the mechanical forces applied to the material during milling. They appear at the macroscopic level as changes in interplanar distances, as shown in Table 6, and therefore affect the lattice parameters. Consequently, the diffraction peaks shift, as observed in the X-ray diffraction spectra shown in Figures 18, 19.

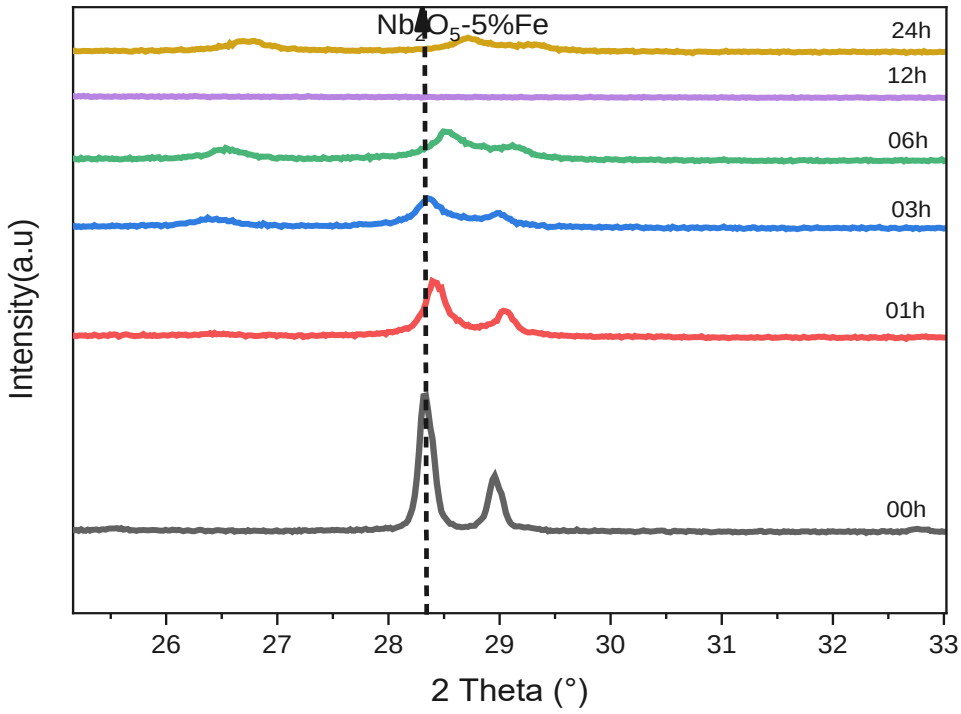

Figure 16: Evolution of the most intense peaks as a function of milling time

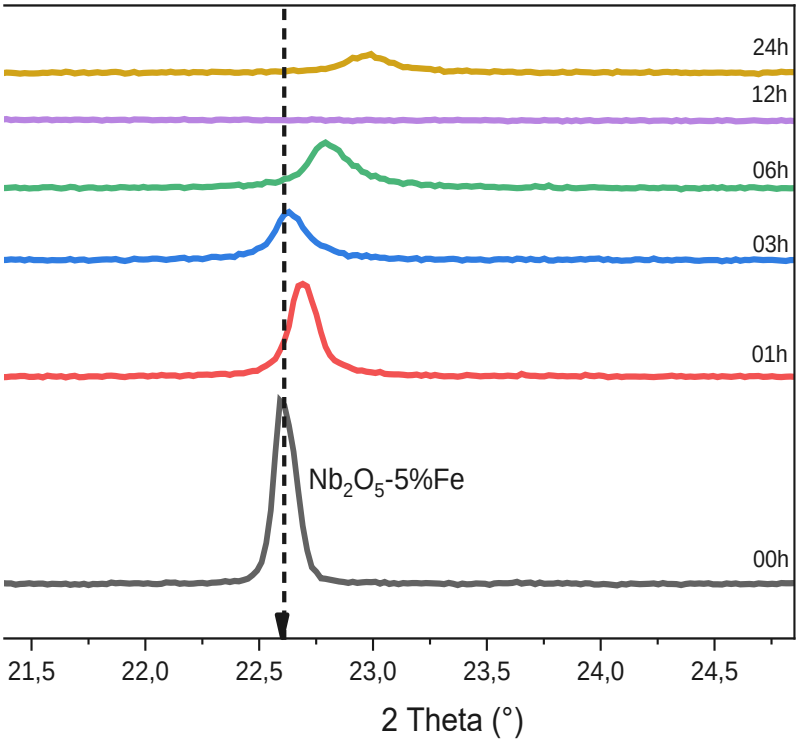

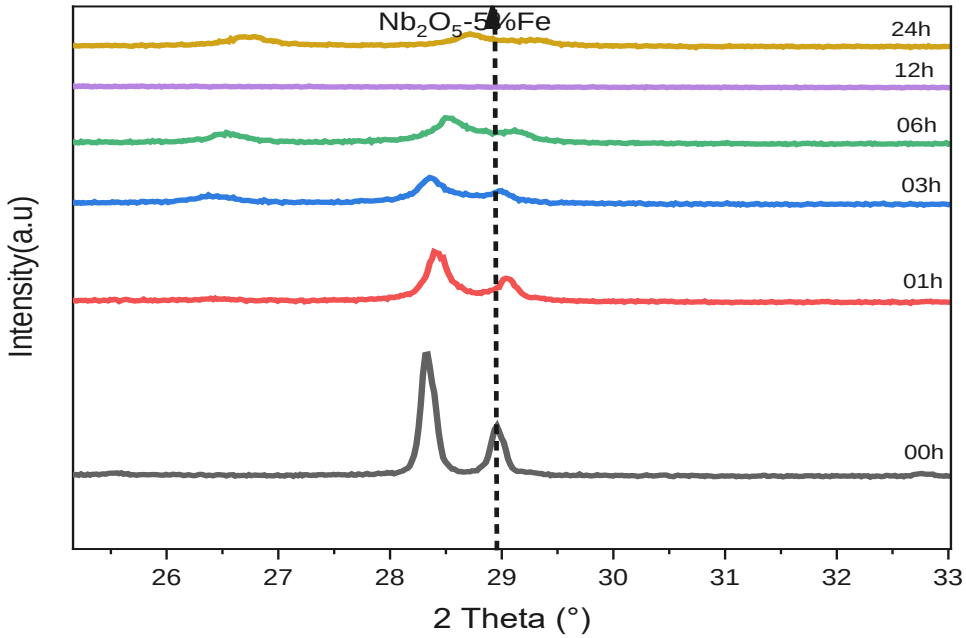

Figure 17: Evolution of the most intence diffraction peaks as a function of milling time

According to A. Esteves et al. [2], first-order internal stresses have a significant effect on the crystal structure of milled materials. They not only modify interplanar distances but may also induce defects and distortions in the crystal lattice. These effects appear as a shift in diffraction peaks, which is an important indicator of structural changes in the material.

The analysis of diffraction peak profiles makes it possible to characterize structural and microstructural imperfections induced by the milling process. There are two categories of structural imperfections or effects that can significantly modify the diffraction peak profile: the size effect and the distortion effect.

The size effect is related to the reduced dimension of the crystallites. When crystallite size decreases, diffraction peaks broaden. This peak broadening is due to the finite size of the crystallites, which limits diffraction coherence.

The distortion effect is associated with deformations of the crystal lattice. These deformations may be caused by internal stresses or dislocations, which disturb the crystalline order and lead to variations in interplanar distances. These results in peak broadening and peak shifting.

The results presented in Tables 7 and 8 for microstrain and dislocation density, which are key structural parameters in crystal lattices generally determined from

the broadening of X-ray diffraction peaks and calculated using the Williamson–Hall method, confirm the effects mentioned above.

The phenomena of peak shift and peak broadening are explained by Tables 7 and 8, which show the effect of milling on the increase in microstrain values, measuring local variations in the crystal lattice, while dislocation density quantifies the length of defect lines per unit volume.

Table 7 Variation of microstrain as a function of milling time

Milling time (h)	Microstrain $\varepsilon \times 10^{-3}$
0	1.92854
1	2.37531
3	2.20526
6	2.66419
24	3.36074

Table 8 Dislocation density as a function of milling time

Milling time (h)	Dislocation density $\delta \times 10^{-4}$
0	134.62
1	165.557
3	155.39
6	186.432
24	249.697

By combining the analysis of these effects, detailed information can be obtained on the structural and microstructural characteristics of the samples, such as crystallite size and the level of internal stresses. This information is essential for understanding the impact of the milling process on the studied materials.

2.1. Structural Properties

Pure Nb_2O_5 exists in several polymorphic forms (T, M, H, etc.). The introduction of 5% iron induces significant changes in the crystal lattice.

Substitution and ionic radius: The Fe^{3+} ion, with an ionic radius of approximately 0.645 Å, generally substitutes for Nb^{5+} ions, whose radius is approximately 0.64 Å, because of the similarity in size.

Lattice distortion: Although the radii are close, the valence difference (+3 compared with +5) creates local stresses. A slight contraction of the lattice parameters (a, b, c), detectable by X-ray diffraction, is often observed. Doping with a lower-valence cation (Fe^{3+} for Nb^{5+}) requires charge compensation.

Crystalline impact: The creation of oxygen vacancies (V_O) causes local relaxation of the structure. These vacancies allow neighboring ions to move slightly from their ideal positions, thus modifying the lattice parameters in a nonlinear way.

Solubility limits: At 5%, iron is generally well incorporated into the Nb_2O_5 structure. However, if the synthesis is not optimal, traces of secondary phases such as $FeNb_2O_6$ may appear.

Point defects: To maintain electroneutrality, the incorporation of Fe^{3+} often generates oxygen vacancies (V_O), modifying the stoichiometric balance of the crystal.

These structural defects, such as vacancies and interstitial atoms, can form defect energy levels within the band gap that trigger low-energy electronic transitions. This proves that V_O vacancies are abundant in the material and leads to a decrease in the optical band gap [3].

2.2. Microstructural Properties

According to several studies [4, 5, 6], microstructure concerns the arrangement of grains and the surface morphology, generally observed by scanning electron microscopy (SEM). As reported by several authors [3, 7, 8] in their work on iron-doped niobium pentoxide, the following observations were made:

Crystallite size: Iron doping often tends to inhibit grain growth. Fe ions are located at grain boundaries and act as barriers to atomic diffusion, leading to a finer nanometric structure.

Morphology: The addition of 5% Fe can transform rod-like or spherical structures into more irregular or porous forms, thereby increasing the specific surface area.

Homogeneity: Energy-dispersive X-ray analysis (EDX) can confirm the uniform distribution of iron within the niobium matrix.

3. Evolution of Lattice Parameters and Volume

The evolution of the crystal parameters a, b, and c of the Nb_2O_5 phases in the Nb_2O_5–5% Fe compound during milling from 01 h to 24 h is illustrated in Figure 18. The c parameter, calculated from the (001) plane, decreases from 3.932 Å at 0 h to 3.865 Å at 24 h, indicating a notable reduction along the c axis. The a parameter, calculated from the (200) plane, decreases from 6.1645 Å to 6.088 Å, while the b parameter follows a similar reduction, decreasing from 29.304 Å at 00 h to 28.919 Å at 24 h. Finally, the overall unit-cell volume progressively decreases.

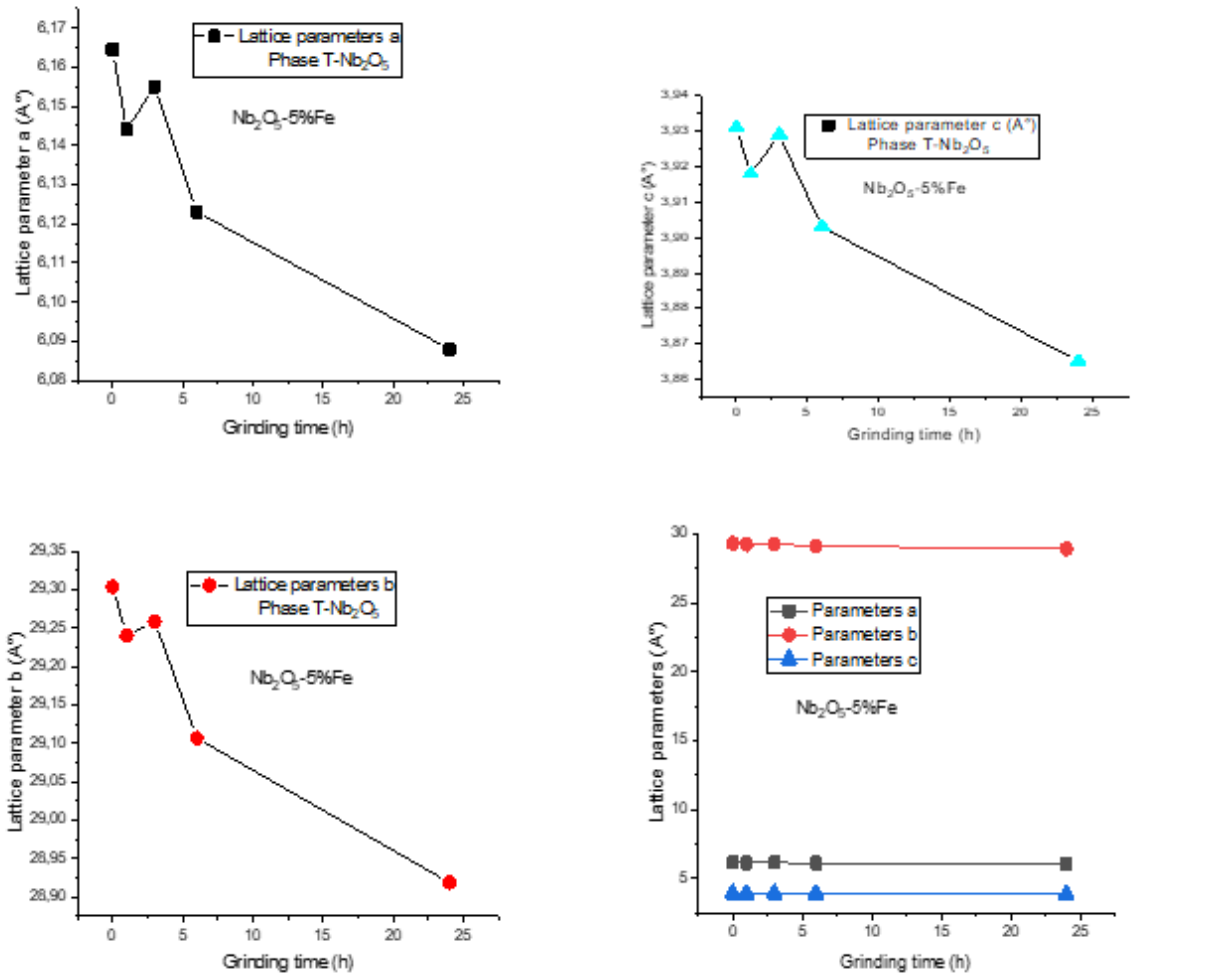

Figure 18 : Variations in the lattice parameters of the T-Nb2O5 phase as a function of milling time

The analysis of these results shows that mechanical milling induces a reduction in atomic distances, that is, a contraction. A volumetric contraction of 4.3% after 24 h is also observed. This strong decrease in volume indicates that milling energy forces the atoms to move closer together and that Fe ions enter the structure, producing compressive distortion of the Nb_2O_5 lattice, as shown in Table 9.

Table 9 : Evolution of lattice parameters and volume

Milling time (h)	a (Å)	b (Å)	c (Å)	Volume (Å3)
0	6.1645	29.304	3.931	710.113
1	6.144	29.24	3.918	703.87
3	6.155	29.259	3.929	707.57
6	6.123	29.107	3.903	695.601
24	6.088	28.919	3.865	680.476

The structural and microstructural study of the Nb_2O_5 system doped with 5% iron by mechanosynthesis reveals profound transformations within the crystal lattice during 24 hours of treatment. The results in Table 9 show that increasing the milling time from 01 h to 24 h induces a systematic contraction of the lattice parameters (a, b, c). The unit-cell volume decreases by about 4.3%, from 710.11 Å3 to 680.47 Å3. This phenomenon reflects the forced insertion of Fe^{3+} ions into the niobium matrix and local densification under the effect of high-energy mechanical impacts.

It can be concluded that, unlike conventional thermal substitutional doping, which often expands the lattice, mechanical milling with 5% Fe appears to cause compression of the lattice. This can be explained by the forced insertion of iron into interstitial sites or by a reduction in interatomic distances caused by the high local pressures generated during ball impacts.

After 24 h, the material is in a highly strained nanocrystalline state. The lattice is compressed along the three axes, indicating a high density of defects, such as dislocations and vacancies.

4. Microstructural Analysis

Figure 19 shows the variations in average grain size (D) with milling time. As shown in the figure, the grain size of the Nb_2O_5 phase decreases progressively with increasing milling time, from 75.1632 nm at 00 h to 42.1514 nm after 24 h of milling.

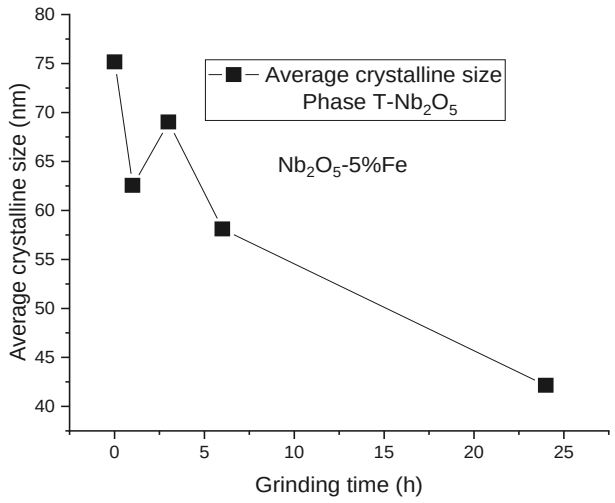

Figure 19: Evolution of average crystallite size as a function of milling time

This reduction in grain size is a direct consequence of mechanical milling mechanisms, in which repeated impacts and shear forces break the grains into smaller particles. As milling time increases, the mechanical energy supplied promotes fragmentation and grain refinement, leading to a reduced grain size.

Figure 20 (a, b) presents the evolution of microstrain ($<\sigma 2>^{1/2}$) and dislocation density determined by the Williamson–Hall method. This analysis includes the crystallographic T-Nb_2O_5 phases.

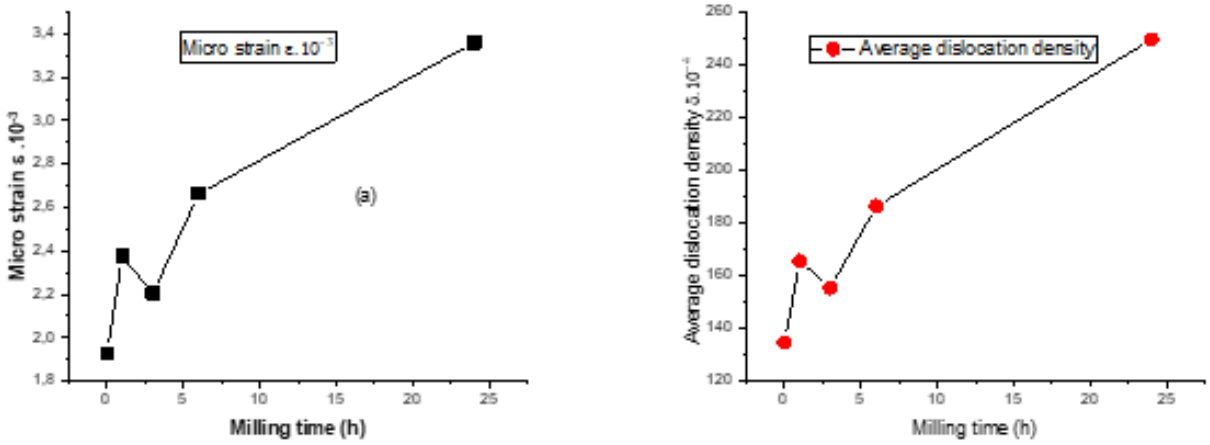

Figure 20: Evolutions (a) microstrain (ε ou $<\sigma 2>^{1/2}$ (%)) , et (b) dislocations density δ (m^{-2}) in Nb_2O_5-5%Fe phases as a fonction of milling time

When grain size decreases during the milling process, an increase in the microstrain rate in the T-Nb_2O_5 phases and in dislocation density is simultaneously observed. The mechanical stresses induced by milling introduce crystalline defects and dislocations, contributing to lattice deformation. These imperfections increase the distortion of the crystal lattice, which is also reflected in the variations in diffraction parameters observed in the X-ray spectra.

On the other hand, this decrease in grain size is associated with an increase in microstresses and dislocation density, as shown in Figure 20 (a) and (b).

Thus, the structural and microstructural study of Nb_2O_5 doped with 5% Fe is based on understanding how iron ions enter the niobium oxide lattice. Fe^{3+} (radius = 0.64 Å) has a size close to that of Nb5+ (radius = 0.64 Å in octahedral coordination). At 5%, iron replaces niobium in the NbO_6 octahedral sites. Despite the similarity in size, the difference in charge (3+ versus 5+) creates local stresses

and a contraction of the lattice parameters (a, b, c), leading to lattice distortion. To maintain crystal electroneutrality after replacing Nb^{5+} with Fe^{3+}, the lattice generates oxygen vacancies (V_O). These vacancies increase structural disorder, which is visible through the broadening of X-ray diffraction peaks.

To clearly illustrate the relationship between the different parameters, Table 10 presents the variations of D, ε, and δ as a function of milling time.

Table 10 D, ε, and δ as a function of milling time

Milling time (h)	Crystallite size D (nm)	Microstrain ε × 10−3	Dislocation density δ × 10−4
0	75.16329516	1.92854	134.62
1	62.56175851	2.37531	165.557
3	69.03717873	2.20526	155.39
6	58.11148725	2.66419	186.432
24	42.15148435	3.36074	249.697

The phenomenon of iron insertion into the niobium pentoxide matrix can be summarized as follows:

Property	Effect of doping (5% Fe)	Main cause
Structure	Slight lattice distortion	Fe^{3+} / Nb^{5+} substitution
Phase	Possible appearance of V_O	Charge compensation
Grain size	Decrease	Growth inhibition at grain boundaries

5. Chapter Conclusion

Nanostructured powders of niobium pentoxide Nb_2O_5 doped with 5% iron Fe were successfully prepared using a P4 planetary mill for different milling times ranging from 1 h to 24 h. The obtained powders were characterized by X-ray diffraction (XRD).

The study of structural properties was carried out using X-ray diffraction. From the XRD spectra, it was found that the structural and microstructural study of Nb2O5 doped with 5% Fe depends on understanding how iron ions enter the niobium oxide lattice.

According to the XRD results, the crystallographic evolution shows a systematic contraction of the lattice parameters (a, b, c). The unit-cell volume decreases by 4.3%. This phenomenon reflects the forced insertion of Fe3+ ions

into the niobium matrix and local densification under the effect of high-energy mechanical impacts.

General Conclusions

General Conclusions

- Nanostructured Nb_2O_5–5% Fe samples were prepared by the milling technique using a PM 400 Retsch vibratory planetary ball mill.
- The Nb_2O_5 and Fe powders were prepared and weighed in precise proportions inside a glove box and introduced into jars under nitrogen. The selection of the balls and jars was made to reduce contamination caused by ball–powder and powder–jar wall impacts. Mechanosynthesis was carried out in the planetary mill at a rotation speed of 350 rpm. To avoid excessive heating during milling, each 60 min of milling was followed by a 30 min stop. The selected milling times were 1, 3, 6, 12, and 24 hours.
- The structural and microstructural characterization of the samples was performed by X-ray diffraction using X'PertHighScore and Origin Pro programs.
- X-ray structural analysis of the Nb_2O_5–5% Fe samples shows that, after 03 h of milling, the X-ray diffraction patterns of all samples have similar shapes. However, they differ in peak intensity and angular position.
- It was also observed after 03 h of milling that the iron peaks completely disappear and that iron is inserted into the Nb2O5 matrix.
- The complete disappearance of the iron peaks is accompanied by a shift of the peaks toward higher angles. This angular shift is clearly visible in the X-ray diffraction spectra and is strong evidence that iron atoms have dissolved into the Nb_2O_5 crystal lattice.
- The angular shift of the diffraction peaks observed in the spectra may also be attributed to first-order internal stresses, or microdistortions, induced by the milling process.
- The broadening of the diffraction peaks (FWHM) confirms a drastic reduction in the size of coherent diffraction domains. The material evolves toward a nanocrystalline state characterized by a high density of internal microstrains.
- The evolution of the lattice parameters a, b, and c of the Nb_2O_5 phases in the Nb_2O_5–5% Fe mixture during milling shows low and decreasing values, reaching the nanometric range, which is characteristic of parameter contraction and unit-cell volume reduction. This phenomenon reflects the forced insertion of Fe^{3+} ions into the niobium matrix and local densification under the effect of high-energy mechanical impacts.

General Conclusions

- After 24 h, the material is in a highly strained nanocrystalline state. The lattice is compressed along the three axes, indicating a high density of defects, including dislocations and vacancies.

- The microstructural study showed that the grain size of the Nb_2O_5-5%Fe phase progressively decreases with increasing milling time, from 75.163 nm at 0 h to 42.151 nm after 24 h of milling. This reduction in grain size is a direct consequence of mechanical milling mechanisms, which lead to nanostructuring.
- The analysis of peak positions (2θ) shows a systematic shift toward higher angles as milling time increases.
- The analysis of the spectra of milled powders for phase identification and Rietveld refinement using X'PertHighScore shows that, from 03 h of milling, traces of secondary phases appear and are identified as the $FeNb_2O_6$ phase, characteristic of non-optimal synthesis. However, these peaks are weak and symmetric.
- By comparison with other studies, it appears that lattice contraction and iron insertion modify the periodic potential of the crystal. The optical gap (Eg) should decrease significantly, making the compound active under visible light.
- The synergy between structural distortion and the introduction of iron energy levels suggests a significant reduction in band-gap energy. The final compound presents optimal characteristics for photocatalytic applications under visible light, benefiting from both broader absorption and a large specific surface area.
- A milling time of 24 h makes it possible to obtain the most intimate mixture between iron and niobium, but at the cost of strong degradation of crystallinity. If the objective is photocatalysis, the 06 h compound may offer a better compromise between a stable crystalline structure and good dopant incorporation.
- Mechanical milling for 24 h makes it possible to synthesize a metastable solid solution of Nb_2O_5 that would be difficult to obtain by a conventional thermal route. For applications requiring a compromise between crystallinity and doping, an intermediate milling time of around 6 h appears to provide the most balanced structure.